Journal of Solid Mechanics Vol. 15, No. 2 (2023) pp. 120-143
DOI: 10.22034/jsm.2021.1937989.1713

Research Paper

Nonlinear Free Vibration Analysis of Functionally Graded Sandwich Beam with Magnetorheological Fluid Core Using Timoshenko Beam Theory

O. Miraliyari, S. Jafari Mehradadi *, M.M. Najafizadeh

Department of Mechanical Engineering, Islamic Azad University, Arak Branch, Arak, Iran

Received 10 February 2023; accepted 25 March 2023

ABSTRACT

In this paper, the analysis of nonlinear free vibrations of beams made of functionally graded materials with magnetorheological fluid as core is investigated. It is assumed that the beam is made of three layers including constraining layer, magnetorheological fluid and base layer and is located on Simply-Simply, Clamped-Simply and Clamped–Clamped supports. The governing equations of the beam are derived using the Hamilton's principle. To obtain the vibrational frequencies, the theory of Timoshenko beam is used by the Generalized Differential Quadrature method. The effects of magnetic field intensity, power law exponents, core thickness and constraining layer thickness and the length of the beam on natural frequency and modal loss factor related to different frequencies modes for the three boundary conditions have been investigated. The results show the effects of physical and geometrical parameters regarding the natural frequency and modal loss factor of the sandwich beam with different modes. Also, the frequency and loss factor values obtained from Generalized Differential Quadrature method are very close to the results obtained by the Finite Element method. This shows the accuracy and precision of this method.

Keywords : Nonlinear free vibration; Functionally graded sandwich beam; Magnetorheological fluid core; Euler Bernoulli and Timoshenko beam theories.

1 INTRODUCTION

SMART materials are materials whose properties change significantly in the absence of external stimulus. So far, many smart materials have been identified, the most important of which are magnetorheological fluids, electrorheological fluids, piezoelectric materials and shape-memory alloys. Magnetic suspensions are mixed fluids whose rheological properties change significantly in the presence of a magnetic field [1]. Many studies on MR and

*Corresponding author. Tel.: +98 86 33412563; Fax: ++98 86 33412563.
E-mail address: s-jafari@iau-arak.ac.ir (S. Jafari Mehradadi)

ER materials have been reported in this article. In 2014, Allahverdizadeh and et al [2] analyzed the nonlinear vibrations of functional sandwich beams with electrorheological fluid. This paper investigates the dynamic characteristics related to the amplitude of functional sandwich beams with electro-rheological fluid. The nonlinear characteristics of the electrorheological fluid layer (ERF) are modeled by an exponential function. In addition, due to the nonlinearity of the geometry and the assumption of continuous change for the properties of the functional calibrated material (FGM) in the direction of the layer thickness, the nonlinear governing equations for free vibration of the FGER beam are obtained by finite element method. Aguib and et al [3] studied numerical simulations of the nonlinear static behavior of composite sandwich beams with magnetorheological fluid cores. In this paper, the static behavior of magnetorheological elastomer sandwich beams in bending mode with cross-section was studied. The beam consists of two aluminum shells that surround a core of silicon oil and is loaded with 30% iron particles. Beam stiffness is created by adding a typical stiffness matrix of two aluminum shells and a mixed MRE stiffness matrix. Then a function of the magnetorheological properties of MRE is presented. Dynamic behavior of sandwich beams with different compositions of magnetorheological fluid core investigated by Subash Acharya and et al [4]. In this paper, six samples of magnetorheological fluid including a combination of two particles and three weight components of carbonyl iron powder have been studied. A sandwich beam with MRF 132DG fluid as core was used to analyze viscoelastic characteristics of beam. Biswajit Nayak and et al [5] analyzed the capabilities of a three-layered magnetorheological viscoelastic cored sandwich beam with conductive and non-conductive skins. To mathematical modeling of magnetorheological sandwich beam, finite element method is used. The results obtained by FEM method were compared with the results obtained from experiments on sandwich beams with viscoelastic core. Navazi and et al [6] investigated the free vibration of a magnetorheological rotating sandwich beam with a tapered cross section. The geometry of the beam consists of two elastic layers between which a magnetoreological fluid is placed. The equations of motion of the beam are based on Euler-Bernoulli theory. Using the Lagrange equation the governing equations are discretized based on the Ritz method. Dynamic analysis of an axially moving sandwich beam with a polyurethane core as a viscoelastic core and two aluminum facings as elastic faces is studied by Krzysztof Marynowski [7]. In this paper only shear deformation is considered in the core. Material characteristics of the core are modeled with Kelvin–Voigt rheological model. For solving the governing equation the Galerkin method is used. The vibration characteristics of electrorheological elastomer cantilever sandwich beams were analyzed by Kexiang Wei and et al [8]. In this work characteristics and control capabilities of the beam subjected to different electric fields are investigated. The finite element method was used to investigate the frequency response of the beam vibrations. Also, experimental analysis was performed to evaluate the effects of electric field on the frequency responses and natural frequencies of sandwich beams. Allahverdizadeh and et al [9] investigated vibration characteristics of a rotating Functionally Graded Electro-Rheological (FGER) beam. The beam consists of three layers so that the electro-rheological fluid is located between two elastic layers of functionally graded materials. In beam analysis, the classical beam theory method has been used. The Hamilton principle and the finite element method have also been used to obtain the equations of motion of the beam. Dynamic behavior of functionally graded electrorheological sandwich beams is studied by Allahverdizadeh and et al [10]. The beam consists of constraining layers that are made of functionally graded materials (FGM) and middle layer that is electro-rheological fluid (ERF). The finite element method (FEM) is used to obtain the equations of motion of the beam. Liao-Liang Ke and et al [11], Elmaguiri and et al [12] and Sompon Taeprasartsit [13] studied nonlinear vibration of beams made of functionally graded materials (FGM). Euler-Bernoulli beam theory and von-Kármán geometric nonlinearity are used to obtain the equations of motion of the beam. Sheng and et al [14] investigated nonlinear vibration of functionally graded beams subjected to parametric and external excitations. In this article, equations of motion are derived based on the Hamilton's principle, Euler-Bernoulli beam theory and von-Kármán geometric nonlinearity. Other methods such as variational iteration (VIM) and parameterized perturbation (PPM) methods were also used to study the nonlinear vibrations of the Bernoulli Euler beam [15]. Sümeyye Sınır and et al [16] investigated nonlinear free and forced vibrations of functionally graded beams with non-uniform cross-section. Euler-Bernoulli beam theory is used to derive beam motion equations. Hemmatinezhad and et al [17] and Jagadish Babu Gunda [18] analyzed the nonlinear free vibration analysis of functionally graded beams. The von-Karman type nonlinear strain–displacement relationships are employed based on the Timoshenko beam theory.The large-amplitude nonlinear vibration of functionally graded (FG) beams made of porous material is analyzed by Farzad Ebrahimi and et al [19] and Da Chen and et al [20]. The governing equations are derived based on Timoshenko beam theory through Hamilton's principle and to solve the governing equations Galerkin's method and the method of multiple scales have been applied. In many studies on beam vibrations, in addition to the FEM method, the generalized differential quadrature (GDQ) method has been used. Ghorbanpour Arani and et al [21] examined nonlinear thermo free vibration and instability of viscose fluid-conveying double-walled carbon nanocones (DWCNCs). The governing equations are solved using Hamilton’s principle and differential quadrature method. The

nanocone is simulated as a clamped-clamped Euler-Bernoulli's beam located in an elastic foundation of the Winkler and Pasternak type. In this regard, Ghaitani and et al [22] investigated nonlinear vibration and instability response of an oil pipe located on an elastic foundation. The governing equations are derived based on Timoshenko beam theory. The von-Karman type nonlinear strain–displacement relationships are employed. The governing equations are solved using a direct iterative approach and Hamilton's principle. The differential quadrature method (GDQ) is used to obtain the nonlinear vibration frequencies and critical fluid velocity of the pipe.

In this paper, nonlinear free vibrations of a FGMR beam are formulated and verified by associated studies in the literature. Hamilton's principle, the theory of Timoshenko beams and GDQ method are used to derive vibrational frequencies. The effects of magnetic field intensity, power law exponents, core thickness and constraining layer thickness and the length of the beam on natural frequency and modal loss factor related to different frequencies modes for the three mentioned SS, CS and CC boundary conditions have been investigated.

2 PROBLEM DESCRIPTIONS

2.1 Description of functionally graded sandwich beam with magnetorheological fluid core

The sandwich beam model is described based on the following hypotheses:

1. Top and bottom layers are considered as ordinary beams with axial and bending resistance.
2. The core layer does not withstand any longitudinal stress if it withstands nonlinear displacement fields along the x and z axes.
3. All the three layers are assumed to be perfectly bonded and there is no slippage between the layers.
4. The transverse displacements of the top and bottom layers are equal to the transverse displacements of the core at interfaces.

The sandwich beam consists of upper and lower layers of functionally graded linear elastic material with thickness h_1 and h_3 and a core of viscoelastic material with thickness h_2. The magnetorheological sandwich beam model is shown in Fig.1.

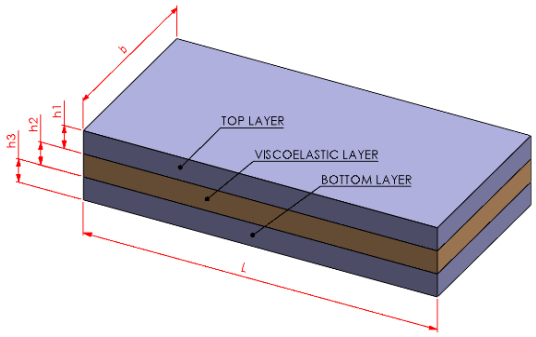

Fig.1
The MR fluid layer sandwich beam.

2.2 Structural relationships of MR fluid

To understand and predict the behavior of a MR fluid, it must be possible to model the fluid mathematically. Intelligent liquids have a low viscosity in the absence of magnetic applications, but they become quasi-solid as a result of the application of a magnetic field. The yield stress depends on the magnetic field applied to the liquid, but as the magnetic field increases, we reach a point where the intensity of the magnetic field has no greater effect and the liquid becomes magnetically saturated at this point. Therefore, the behavior of magnetorheological fluid (MR) can be assumed to be similar to Bingham Plastic. However, a magnetorheological fluid does not exactly follow Bingham plastic properties. For the following example, the fluid yield stress in the active state behaves like a viscoelastic material with a complex shear modulus that is a function of the magnetic field strength. (Fig. 2)

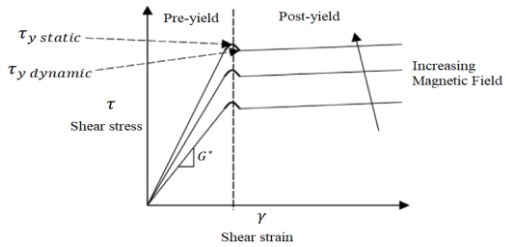

Fig.2
Shear stress–shear strain relationship of MR materials under varying intensities of magnetic field [23].

Since the MR material has linear viscoelastic properties in the pre-yield regime, the shear modulus is complex in shape and depends on the magnetic field intensity. The complex shear modulus for viscoelastic materials is expressed as follows. [6,8]

$$\tau = G^* \gamma \tag{1}$$

$$G^* = G' + iG'' = G'\left(1 + i\,\frac{G''}{G'}\right) = G'(1 + i\,\eta) \tag{2}$$

where τ is the shear stress, γ is the shear strain and G^* is the complex shear modulus. In this regard, G' is called the shear modulus of storage and indicates the material ability to store elastic strain energy during a deformation cycle. The imaginary part of G'', is called the shear modulus of dissipation and is associated with energy dissipation during deformation. On the other hand, the loss modulus is a measure of the energy dissipated per unit volume of the material over a cycle. G''/G' is the energy dissipation coefficient of the structure denoted by η.

The complex shear modulus for the MR material is defined as a polynomial function in terms of magnetic field B (in Gaussian terms G) as follows [24].

$$G^* = G' + iG'' \tag{3a}$$

$$G'(B) = -3.3691B^2 + 4.9975\times10^3 B + 0.873\times10^6 \tag{3b}$$

$$G''(B) = -0.9B^2 + 0.8124\times10^3 B + 0.1855\times10^6 \tag{3c}$$

2.3 FGM materials

The material properties P of FGMs are a function of the material properties and volume fractions of the constituent material, and are expressed as follows [9,25].

$$P = \sum_{j=1}^{k} P_j V_{fj} \tag{4}$$

where P_j and V_{fj} are respectively, the material property and volume fraction of the constituent material j. In this paper, it is assumed that the functional layer is a combination of ceramic and metal and the composition changes from one surface to another. The Young's modulus E and the density ρ are defined as a property of P as follows.

$$P = P_c V_c + P_m V_m \tag{5}$$

where c and m indicates respectively ceramic and metal. The volume fractions of all the constituent materials should add up to one, i.e.

$$\sum_{j=1}^{k} V_{fj} = 1 \tag{6}$$

The volume fraction of ceramics and metals is expressed as follows.

$$V_{fc} + V_{fm} = 1 \tag{7}$$

For a beam with a uniform thickness h and a reference surface at its middle surface, the volume fraction can be written as. [12,19]

$$V_f = \left(\frac{2z + h}{2h} \right)^N \tag{8}$$

where N is the power- law exponent, $0 \le N \le \infty$. The mechanical properties of materials according to the law of power are expressed as follows. [9,11,12,19]

$$P(z_i) = (P_c - P_m)(\frac{2z_i + h_i}{2h_i})^N + P_m \quad , \quad i = 1,3 \tag{9}$$

In FGM layers, a combination of aluminum (Al) and zirconium (ZrO_2) is used.

2.4 Displacement field

The longitudinal and transverse displacement fields for the upper and lower layers according to Timoshenko theory are expressed as follows. [2,3,9,10,11,12,19]

$$U_i = u_i(x,t) + z_i \varphi_i(x,t) \text{ , } i = 1,2,3 \tag{10a}$$

$$W_i = w(x,t) \tag{10b}$$

where U_i is the longitudinal displacements of the upper and lower layers for any x and z location. u_i is the longitudinal displacement at the centroid of the upper and lower layers, z_i is the distance from centroid of the upper and lower layers in the transverse direction, W_i is the transverse displacement in the upper and lower layers for any x and z location. w is the transverse displacement at the centroid of the top and bottom layers. φ_i is the angle of rotation of the cross section about the y axis and $i = 1,2,3$ are the coordinates of the top, middle and bottom layers.

As expressed, in those assumptions with a perfect bond between the three layers, to obtain the continuity between all the three layers the following relations are used. [3]

$$U_1(x, -h_1/2, t) = U_2(x, h_2/2, t) \tag{11a}$$

$$U_2(x, -h_2/2, t) = U_3(x, h_3/2, t) \tag{11b}$$

Using the interlayer continuity conditions for Timoshenko theory, the longitudinal displacement at the centroid of the middle layer and the angle of rotation of the cross section are followed as.

$$u_2(x,t) = (\frac{u_1 + u_3}{2}) + \frac{1}{4}(h_3\varphi_3 - h_1\varphi_1) \tag{12a}$$

$$\varphi_2(x,t)=(\frac{u_1-u_3}{h_2})-\frac{1}{2h_2}(h_3\varphi_3+h_1\varphi_1) \tag{12b}$$

2.5 Strain-Displacement relations

It can be easy to formulate the strains developed in all the three layers by using the assumed displacement fields. The mechanical strains of the first and third layers according to Timoshenko theory are obtained as follows. [2,3,11,12,13,14,19]

$$\varepsilon_{xx}=\frac{\partial u_i}{\partial x}+z_i\frac{\partial \varphi_i}{\partial x}+\frac{1}{2}(\frac{\partial w}{\partial x})^2 \tag{13a}$$

$$\varepsilon_{yy}=\varepsilon_{zz}=0 \tag{13b}$$

$$\varepsilon_{xy}=\varepsilon_{yz}=0 \tag{13c}$$

$$\varepsilon_{xz}=\frac{1}{2}\left(\varphi_i+\frac{\partial w}{\partial x}\right) \tag{13d}$$

where $i=1,3$ are the coordinates of the top and bottom layers. The mechanical strains of the second layer are obtained as follows.

$$\varepsilon_{xx}=\varepsilon_{yy}=\varepsilon_{zz}=0 \tag{14a}$$

$$\varepsilon_{xy}=\varepsilon_{yz}=0 \tag{14b}$$

$$\varepsilon_{xz}=(\frac{u_1-u_3}{h_2})-\frac{1}{2h_2}(h_3\varphi_3+h_1\varphi_1)+\frac{\partial w(x,t)}{\partial x} \tag{14c}$$

2.6 Constitutive equations

The relationship between stress and strain according to Hooke's law in the plane stress state is expressed as follows. [9,17,19]

$$\begin{Bmatrix}\sigma_{xx}\\ \sigma_{yy}\\ \sigma_{xz}\end{Bmatrix}=\begin{bmatrix}Q_{11}(z_i) & Q_{12}(z_i) & 0\\ Q_{12}(z_i) & Q_{22}(z_i) & 0\\ 0 & 0 & Q_{55}(z_i)\end{bmatrix}\begin{Bmatrix}\varepsilon_{xx}\\ \varepsilon_{yy}\\ \gamma_{xz}\end{Bmatrix} \tag{15}$$

which Q_{ij} is the stiffness matrix for single layer as follows. [9]

$$Q_{11}(z_i)=Q_{22}(z_i)=\frac{E(z_i)}{1-\nu^2} \tag{16a}$$

$$Q_{12}(z_i)=\frac{\nu E(z_i)}{1-\nu^2} \tag{16b}$$

$$Q_{55}(z_i)=\frac{E(z_i)}{2(1+\nu)} \tag{16c}$$

The components of resulting forces and moments are expressed as follows. [11,13]

$$N_x^{(i)}=\int\sigma_x(z_i)dA_i \tag{17a}$$

$$M_x^{(i)}=\int\sigma_x(z_i)z_i\,dA_i \tag{17b}$$

$$R_{xz}^{(i)}=\int\sigma_{xz}(z_i)dA_i \tag{17c}$$

By substituting relations (13) and (14) in Eqs. (15) and (17), the components of resulting forces and moments in terms of displacements based on Timoshenko theory are expressed as follows. [11,13,14]

$$N_x^{(1)}=A_{11}^{(1)}\left(\frac{\partial u_1(x,t)}{\partial x}+\frac{1}{2}\left(\frac{\partial w(x,t)}{\partial x}\right)^2\right)+B_{11}^{(1)}\left(\frac{\partial\phi_1(x,t)}{\partial x}\right) \tag{18a}$$

$$R_{xz}^{(1)}=A_{55}^{(1)}\left(\phi_1(x,t)+\frac{\partial w(x,t)}{\partial x}\right) \tag{18b}$$

$$M_x^{(1)}=B_{11}^{(1)}\left(\frac{\partial u_1(x,t)}{\partial x}+\frac{1}{2}\left(\frac{\partial w(x,t)}{\partial x}\right)^2\right)-D_{11}^{(1)}\left(\frac{\partial^2\phi_1(x,t)}{\partial x^2}\right) \tag{18c}$$

$$R_{xz}^{2}=A_{55}^{2}\left(-\frac{1}{2}\frac{h_3}{h_2}\phi_3(x,t)+\frac{u_1(x,t)}{h_2}-\frac{1}{2}\frac{h_1}{h_2}\phi_1(x,t)-\frac{u_3(x,t)}{h_2}+\frac{\partial w(x,t)}{\partial x}\right) \tag{18d}$$

$$N_x^{3}=A_{11}^{3}\left(\frac{\partial u_3(x,t)}{\partial x}+\frac{1}{2}\left(\frac{\partial w(x,t)}{\partial x}\right)^2\right)+B_{11}^{3}\left(\frac{\partial\phi_3(x,t)}{\partial x}\right) \tag{18e}$$

$$R_{xz}^{3}=A_{55}^{3}\left(\phi_3(x,t)+\frac{\partial w(x,t)}{\partial x}\right) \tag{18f}$$

$$M_x^{3}=B_{11}^{3}\left(\frac{\partial u_3(x,t)}{\partial x}+\frac{1}{2}\left(\frac{\partial w(x,t)}{\partial x}\right)^2\right)-D_{11}^{3}\left(\frac{\partial^2\phi_3(x,t)}{\partial x^2}\right) \tag{18g}$$

where A_{ij},B_{ij},D_{ij} are the extensional, torsional and flexural stiffness defined as [11,12,13,14,19]

$$A_{ij},B_{ij},D_{ij}=\int_{-\frac{h}{2}}^{+\frac{h}{2}}Q_{ij}(z_i)\;\{1,z,z^2\}\;dz \tag{19}$$

Mass inertia moments are expressed as follows. [11,12,13,19]

$$I_0^i = \int_{-\frac{h_i}{2}}^{\frac{h_i}{2}} \rho_i \, dA_i \tag{20a}$$

$$I_1^i = \int_{-\frac{h_i}{2}}^{\frac{h_i}{2}} \rho_i \, z_i \, dA_i \tag{20b}$$

$$I_2^i = \int_{-\frac{h_i}{2}}^{\frac{h_i}{2}} \rho_i \, z_i^2 \, dA_i \tag{20c}$$

2.7 Equations of motion

To obtain the equations of motion of the beam, we use the Hamilton principle. The advantage of using the Hamilton principle is the possibility of obtaining boundary conditions with equations of motion. [12,13,14]

$$\int_{t_1}^{t_2} \delta L \, dt = \int_{t_1}^{t_2} \delta (T - U) dt = 0 \tag{21}$$

By expanding the variation of kinetic energy T and strain energy U based on Timoshenko theory, the strain energy and kinetic energy of the first and third layers are expressed as follows. [12,13,20]

$$\delta U_i = \int (\sigma_{xx} \delta \varepsilon_{xx} + \sigma_{xz} \delta \gamma_{xz}) dV_i = \int_0^L \int_{A_1} \sigma_{xx} \left[\frac{\partial \delta u_i}{\partial x} + z_i \frac{\partial \delta \varphi_i}{\partial x} + \frac{\partial w}{\partial x} \frac{\partial \delta w}{\partial x} \right] + \sigma_{xz} \left[\delta \varphi_i + \frac{\partial \delta w}{\partial x} \right] dA_i dx \tag{22a}$$

$$\delta T_i = \int_V \rho_i (\dot{U}_i \delta \dot{U}_i + \dot{W}_i \delta \dot{W}_i) dV_i = \int_0^L \int_{A_i} \rho_i \left\{ \left[\dot{u}_i + z_i \dot{\varphi}_i \right] \left[\delta \dot{u}_i + z_i \delta \dot{\varphi}_i \right] + \left[\dot{w} \, \delta \dot{w} \right] \right\} dA_i \, dx \tag{22b}$$

where $i = 1,3$ are the coordinates of the top and bottom layers.

Using the definition of stress consequences, the strain energy changes of the first and third layers are obtained as follows.

$$\delta U_i = \int_0^L \left\{ N_x^i \frac{\partial \delta u_i}{\partial x} + M_x^i \frac{\partial \delta \varphi_1}{\partial x} + N_x^i \left(\frac{\partial w}{\partial x} \frac{\partial \delta w}{\partial x} \right) + R_{xz}^i \left(\delta \varphi_i + \frac{\partial \delta w}{\partial x} \right) \right\} dx \tag{23a}$$

Using the definition of mass moment of inertia, the kinetic energy changes of the first and third layers are obtained as follows.

$$\delta T_i = \int_0^L \left\{ I_0^i (\dot{u}_i \, \delta \dot{u}_i + \dot{w} \, \delta \dot{w}) + I_1^i (\dot{u}_i \, \delta \dot{\varphi}_i + \dot{\varphi}_i \, \delta \dot{u}_i) + I_2^i \, \dot{\varphi}_i \, \delta \dot{\varphi}_i \right\} dx \tag{23b}$$

where $i = 1,3$ are the coordinates of the top and bottom layers.

By expanding the variation of kinetic energy and strain energy, the strain energy and kinetic energy of the second layer are expressed as follows.

$$\delta U_2 = \int [(\sigma_{xz}\delta\varepsilon_{xz})]dV_2 = \int_0^L \int_{A_2} \left\{ \sigma_{xz} \left[(\frac{\delta u_1 - \delta u_3}{h_2}) - \frac{1}{2h_2}(h_3\delta\varphi_3 + h_1\delta\varphi_1) + \frac{\partial\delta w}{\partial x} \right] \right\} dA_2 dx \tag{24a}$$

$$\delta T_2 = \int_V \rho_2(\dot{U}_2\delta\dot{U}_2 + \dot{W}_2\delta\dot{W}_2)dV_2 = \int_0^L \int_{A_2} \rho_2 \left\{ [\dot{u}_2 + z_2\dot{\varphi}_2][\delta\dot{u}_2 + z_2\delta\dot{\varphi}_2] + [\dot{w}\,\delta\dot{w}] \right\} dA_2 dx \tag{24b}$$

Using the definition of stress consequences, the strain energy changes of the second layer are obtained as follows.

$$\delta U_2 = \int_0^L \left\{ R_{xz}^2 (\frac{\delta u_1 - \delta u_3}{h_2}) - \frac{1}{2h_2} R_{xz}^2 (h_3\delta\varphi_3 + h_1\delta\varphi_1) + R_{xz}^2 \frac{\partial\delta w}{\partial x} \right\} dx \tag{25a}$$

Using the definition of mass moment of inertia, the kinetic energy changes of the second layer are obtained as follows.

$$\delta T_2 = \int_0^L \left\{ I_0^2 (\dot{u}_2\,\delta\dot{u}_2 + \dot{w}\,\delta\dot{w}) + I_1^2 (\dot{u}_2\,\delta\dot{\varphi}_2 + \dot{\varphi}_2\,\delta\dot{u}_2) + I_2^2\,\dot{\varphi}_2\,\delta\dot{\varphi}_2 \right\} dx \tag{25b}$$

By integrating Eqs. (23) and (25) in the integration by parts method, the equations of motion in terms of stress components based on Timoshenko theory, are obtained as follows.

$$\begin{aligned} &\frac{\partial \mathrm{N}_x^1}{\partial x} - \frac{R_{xz}^2}{h_2} = I_0^1 \frac{\partial^2 u_1}{\partial t^2} + I_1^1 \frac{\partial^2 \varphi_1}{\partial t^2} + \frac{1}{4} I_0^2 \frac{\partial^2 u_3}{\partial t^2} + \frac{1}{4} I_0^2 \frac{\partial^2 u_1}{\partial t^2} - \frac{1}{8} I_0^2 h_1 \frac{\partial^2 \varphi_1}{\partial t^2} + \frac{1}{8} I_0^2 h_3 \frac{\partial^2 \varphi_3}{\partial t^2} \\ &+ \frac{1}{h_2} I_1^2 \frac{\partial^2 u_1}{\partial t^2} + \frac{1}{(h_2)^2} I_2^2 \frac{\partial^2 u_1}{\partial t^2} - \frac{1}{(h_2)^2} I_2^2 \frac{\partial^2 u_3}{\partial t^2} - \frac{1}{2} I_1^2 \frac{h_1}{h_2} \frac{\partial^2 \varphi_1}{\partial t^2} - \frac{1}{2} I_2^2 \frac{h_3}{(h_2)^2} \frac{\partial^2 \varphi_3}{\partial t^2} - \frac{1}{2} I_2^2 \frac{h_1}{(h_2)^2} \frac{\partial^2 \varphi_1}{\partial t^2} \end{aligned} \tag{26a}$$

$$\begin{aligned} &\frac{\partial \mathrm{N}_x^3}{\partial x} + \frac{R_{xz}^2}{h_2} = I_0^3 \frac{\partial^2 u_3}{\partial t^2} + I_1^3 \frac{\partial^2 \varphi_3}{\partial t^2} + \frac{1}{4} I_0^2 \frac{\partial^2 u_1}{\partial t^2} + \frac{1}{4} I_0^2 \frac{\partial^2 u_3}{\partial t^2} - \frac{1}{8} I_0^2 h_1 \frac{\partial^2 \varphi_1}{\partial t^2} + \frac{1}{8} I_0^2 h_3 \frac{\partial^2 \varphi_3}{\partial t^2} \\ &- \frac{1}{h_2} I_1^2 \frac{\partial^2 u_3}{\partial t^2} - \frac{1}{(h_2)^2} I_2^2 \frac{\partial^2 u_1}{\partial t^2} + \frac{1}{(h_2)^2} I_2^2 \frac{\partial^2 u_3}{\partial t^2} - \frac{1}{2} I_1^2 \frac{h_3}{h_2} \frac{\partial^2 \varphi_3}{\partial t^2} + \frac{1}{2} I_2^2 \frac{h_3}{(h_2)^2} \frac{\partial^2 \varphi_3}{\partial t^2} + \frac{1}{2} I_2^2 \frac{h_1}{(h_2)^2} \frac{\partial^2 \varphi_1}{\partial t^2} \end{aligned} \tag{26b}$$

$$\begin{aligned} &\frac{\partial M_x^1}{\partial x} - R_{xz}^1 + \frac{h_1 R_{xz}^2}{2h_2} = I_1^1 \frac{\partial^2 u_1}{\partial t^2} + I_2^1 \frac{\partial^2 \varphi_1}{\partial t^2} + \frac{1}{4} I_1^2 \frac{(h_1)^2}{h_2} \frac{\partial^2 \varphi_1}{\partial t^2} + \frac{1}{4} I_2^2 (\frac{h_1}{h_2})^2 \frac{\partial^2 \varphi_1}{\partial t^2} + \frac{1}{4} I_2^2 \frac{h_1 h_3}{(h_2)^2} \frac{\partial^2 \varphi_3}{\partial t^2} - \frac{1}{8} I_0^2 h_1 \frac{\partial^2 u_1}{\partial t^2} \\ &- \frac{1}{8} I_0^2 h_1 \frac{\partial^2 u_3}{\partial t^2} + \frac{1}{16} I_0^2 (h_1)^2 \frac{\partial^2 \varphi_1}{\partial t^2} - \frac{1}{16} I_0^2 h_1 h_3 \frac{\partial^2 \varphi_3}{\partial t^2} - \frac{1}{2} I_1^2 \frac{h_1}{h_2} \frac{\partial^2 u_1}{\partial t^2} + \frac{1}{2} I_2^2 \frac{h_1}{(h_2)^2} \frac{\partial^2 u_3}{\partial t^2} - \frac{1}{2} I_2^2 \frac{h_1}{(h_2)^2} \frac{\partial^2 u_1}{\partial t^2} \end{aligned} \tag{26c}$$

$$\begin{aligned} &\frac{\partial M_x^3}{\partial x} - R_{xz}^3 + \frac{h_3 R_{xz}^2}{2h_2} = I_1^3 \frac{\partial^2 u_3}{\partial t^2} + I_2^3 \frac{\partial^2 \varphi_3}{\partial t^2} - \frac{1}{4} I_1^2 \frac{(h_3)^2}{h_2} \frac{\partial^2 \varphi_3}{\partial t^2} + \frac{1}{4} I_2^2 (\frac{h_3}{h_2})^2 \frac{\partial^2 \varphi_3}{\partial t^2} + \frac{1}{4} I_2^2 \frac{h_1 h_3}{(h_2)^2} \frac{\partial^2 \varphi_1}{\partial t^2} + \frac{1}{8} I_0^2 h_3 \frac{\partial^2 u_1}{\partial t^2} \\ &+ \frac{1}{8} I_0^2 h_3 \frac{\partial^2 u_3}{\partial t^2} + \frac{1}{16} I_0^2 (h_3)^2 \frac{\partial^2 \varphi_3}{\partial t^2} - \frac{1}{16} I_0^2 h_1 h_3 \frac{\partial^2 \varphi_1}{\partial t^2} - \frac{1}{2} I_1^2 \frac{h_3}{h_2} \frac{\partial^2 u_3}{\partial t^2} + \frac{1}{2} I_2^2 \frac{h_3}{(h_2)^2} \frac{\partial^2 u_3}{\partial t^2} - \frac{1}{2} I_2^2 \frac{h_3}{(h_2)^2} \frac{\partial^2 u_1}{\partial t^2} \end{aligned} \tag{26d}$$

$$\frac{\partial \mathrm{R}_{xz}^1}{\partial x} + \frac{\partial \mathrm{R}_{xz}^2}{\partial x} + \frac{\partial \mathrm{R}_{xz}^3}{\partial x} + \frac{\partial}{\partial x}\left(\mathrm{N}_x^1 \frac{\partial w}{\partial x} \right) + \frac{\partial}{\partial x}\left(\mathrm{N}_x^3 \frac{\partial w}{\partial x} \right) = I_0^1 \frac{\partial^2 w}{\partial t^2} + I_0^2 \frac{\partial^2 w}{\partial t^2} + I_0^3 \frac{\partial^2 w}{\partial t^2} \tag{26e}$$

Substituting Eqs. (18) in Eqs. (26), the equations of motion in terms of displacement components based on Timoshenko theory, are obtained as follows.

$$A_{11}^{(1)}\left(\frac{\partial^2 u_1(x,t)}{\partial x^2}\right)+A_{11}^{(1)}\left(\frac{\partial w(x,t)}{\partial x}\right)\left(\frac{\partial^2 w(x,t)}{\partial x^2}\right)+B_{11}^{(1)}\left(\frac{\partial^2 \phi_1(x,t)}{\partial x^2}\right)-\frac{A_{55}^{(2)}h_3}{2h_2^2}\phi_3(x,t)-\frac{A_{55}^{(2)}}{h_2^2}u_1(x,t)$$
$$+\frac{A_{55}^{(2)}h_1}{2h_2^2}\phi_1(x,t)+\frac{A_{55}^{(2)}}{h_2^2}u_3(x,t)-\frac{A_{55}^{(2)}}{h_2}\left(\frac{\partial w(x,t)}{\partial x}\right)=I_0^{(1)}\left(\frac{\partial^2 u_1(x,t)}{\partial t^2}\right)-I_1^{(1)}\left(\frac{\partial^2 \phi_1(x,t)}{\partial t^2}\right)$$
$$-\frac{1}{8}I_0^{(2)}h_1\left(\frac{\partial^2 \phi_1(x,t)}{\partial t^2}\right)+\frac{1}{8}I_0^{(2)}h_3\left(\frac{\partial^2 \phi_3(x,t)}{\partial t^2}\right)+\frac{I_1^{(2)}}{h_2}\left(\frac{\partial^2 u_1(x,t)}{\partial t^2}\right)+\frac{I_2^{(2)}}{h_2^2}\left(\frac{\partial^2 u_1(x,t)}{\partial t^2}\right)-\frac{I_2^{(2)}}{h_2^2}\left(\frac{\partial^2 u_3(x,t)}{\partial t^2}\right)$$
$$-\frac{I_1^{(2)}h_1}{2h_2}\left(\frac{\partial^2 \phi_1(x,t)}{\partial t^2}\right)-\frac{I_2^{(2)}h_3}{2h_2^2}\left(\frac{\partial^2 \phi_3(x,t)}{\partial t^2}\right)-\frac{I_2^{(2)}h_1}{2h_2^2}\left(\frac{\partial^2 \phi_1(x,t)}{\partial t^2}\right)+\frac{1}{4}I_0^{(2)}\left(\frac{\partial^2 u_1(x,t)}{\partial t^2}\right)+\frac{1}{4}I_0^{(2)}\left(\frac{\partial^2 u_3(x,t)}{\partial t^2}\right) \quad (27a)$$

$$A_{11}^{(3)}\left(\frac{\partial^2 u_3(x,t)}{\partial x^2}\right)+A_{11}^{(3)}\left(\frac{\partial w(x,t)}{\partial x}\right)\left(\frac{\partial^2 w(x,t)}{\partial x^2}\right)-B_{11}^{(3)}\left(\frac{\partial^2 \phi_3(x,t)}{\partial x^2}\right)-\frac{A_{55}^{(2)}h_3}{2h_2^2}\phi_3(x,t)+\frac{A_{55}^{(2)}}{h_2^2}u_1(x,t)$$
$$-\frac{A_{55}^{(2)}h_1}{2h_2^2}\phi_1(x,t)-\frac{A_{55}^{(2)}}{h_2^2}u_3(x,t)+\frac{A_{55}^{(2)}}{h_2}\left(\frac{\partial w(x,t)}{\partial x}\right)=I_0^{(3)}\left(\frac{\partial^2 u_3(x,t)}{\partial t^2}\right)+I_1^{(3)}\left(\frac{\partial^2 \phi_3(x,t)}{\partial t^2}\right)$$
$$-\frac{1}{8}I_0^{(2)}h_1\left(\frac{\partial^2 \phi_1(x,t)}{\partial t^2}\right)+\frac{1}{8}I_0^{(2)}h_3\left(\frac{\partial^2 \phi_3(x,t)}{\partial t^2}\right)-\frac{I_1^{(2)}}{h_2}\left(\frac{\partial^2 u_3(x,t)}{\partial t^2}\right)-\frac{I_2^{(2)}}{h_2^2}\left(\frac{\partial^2 u_1(x,t)}{\partial t^2}\right)+\frac{I_2^{(2)}}{h_2^2}\left(\frac{\partial^2 u_3(x,t)}{\partial t^2}\right)$$
$$-\frac{I_1^{(2)}h_3}{2h_2}\left(\frac{\partial^2 \phi_3(x,t)}{\partial t^2}\right)+\frac{I_2^{(2)}h_1}{2h_2^2}\left(\frac{\partial^2 \phi_1(x,t)}{\partial t^2}\right)+\frac{I_2^{(2)}h_3}{h_2^2}\left(\frac{\partial^2 \phi_3(x,t)}{\partial t^2}\right)+\frac{1}{4}I_0^{(2)}\left(\frac{\partial^2 u_1(x,t)}{\partial t^2}\right)+\frac{1}{4}I_0^{(2)}\left(\frac{\partial^2 u_3(x,t)}{\partial t^2}\right) \quad (27b)$$

$$B_{11}^{(1)}\left(\frac{\partial^2 u_1(x,t)}{\partial x^2}\right)+B_{11}^{(1)}\left(\frac{\partial w(x,t)}{\partial x}\right)\left(\frac{\partial^2 w(x,t)}{\partial x^2}\right)+D_{11}^{(1)}\left(\frac{\partial^2 \phi_1(x,t)}{\partial x^2}\right)-A_{55}^{(1)}\phi_1(x,t)-A_{55}^{(1)}\left(\frac{\partial w(x,t)}{\partial x}\right)$$
$$-\frac{A_{55}^{(2)}h_1h_3}{4h_2^2}\phi_3(x,t)+\frac{A_{55}^{(2)}h_1}{2h_2^2}u_1(x,t)-\frac{A_{55}^{(2)}h_1}{2h_2^2}u_3(x,t)-\frac{A_{55}^{(2)}h_1^2}{4h_2^2}\phi_1(x,t)+\frac{A_{55}^{(2)}h_1}{2h_2}\left(\frac{\partial w(x,t)}{\partial x}\right)=I_1^{(1)}\left(\frac{\partial^2 u_1(x,t)}{\partial t^2}\right)$$
$$+I_2^{(2)}\left(\frac{\partial^2 \phi_1(x,t)}{\partial t^2}\right)-\frac{1}{16}I_0^{(2)}h_1h_3\left(\frac{\partial^2 \phi_3(x,t)}{\partial t^2}\right)-\frac{I_1^{(2)}h_1}{2h_2}\left(\frac{\partial^2 u_1(x,t)}{\partial t^2}\right)+\frac{I_1^{(2)}h_1^2}{4h_2}\left(\frac{\partial^2 \phi_1(x,t)}{\partial t^2}\right)-\frac{I_2^{(2)}h_1}{2h_2^2}\left(\frac{\partial^2 u_1(x,t)}{\partial t^2}\right)$$
$$+\frac{I_2^{(2)}h_1^2}{4h_2^2}\left(\frac{\partial^2 \phi_1(x,t)}{\partial t^2}\right)+\frac{I_2^{(2)}h_1}{2h_2^2}\left(\frac{\partial^2 u_3(x,t)}{\partial t^2}\right)+\frac{I_2^{(2)}h_1h_3}{4h_2^2}\left(\frac{\partial^2 \phi_3(x,t)}{\partial t^2}\right)-\frac{1}{8}I_0^{(2)}h_1\left(\frac{\partial^2 u_3(x,t)}{\partial t^2}\right)-\frac{1}{8}I_0^{(2)}h_1\left(\frac{\partial^2 u_1(x,t)}{\partial t^2}\right)$$
$$+\frac{1}{16}I_0^{(2)}h_1^2\left(\frac{\partial^2 \phi_1(x,t)}{\partial t^2}\right) \quad (27c)$$

$$B_{11}^{(3)}\left(\frac{\partial^2 u_3(x,t)}{\partial x^2}\right)+B_{11}^{(3)}\left(\frac{\partial w(x,t)}{\partial x}\right)\left(\frac{\partial^2 w(x,t)}{\partial x^2}\right)+D_{11}^{(3)}\left(\frac{\partial^2 \phi_3(x,t)}{\partial x^2}\right)-A_{55}^{(3)}\phi_3(x,t)-A_{55}^{(3)}\left(\frac{\partial w(x,t)}{\partial x}\right)$$
$$-\frac{A_{55}^{(2)}h_3^2}{4h_2^2}\phi_3(x,t)+\frac{A_{55}^{(2)}h_3}{2h_2^2}u_1(x,t)-\frac{A_{55}^{(2)}h_3}{2h_2^2}u_3(x,t)-\frac{A_{55}^{(2)}h_1h_3}{4h_2^2}\phi_1(x,t)+\frac{A_{55}^{(2)}h_3}{2h_2}\left(\frac{\partial w(x,t)}{\partial x}\right)=I_1^{(3)}\left(\frac{\partial^2 u_3(x,t)}{\partial t^2}\right)$$
$$+I_2^{(3)}\left(\frac{\partial^2 \phi_3(x,t)}{\partial t^2}\right)+\frac{1}{16}I_0^{(2)}h_3^2\left(\frac{\partial^2 \phi_3(x,t)}{\partial t^2}\right)-\frac{I_2^{(2)}h_3}{2h_2^2}\left(\frac{\partial^2 u_1(x,t)}{\partial t^2}\right)-\frac{I_1^{(2)}h_3^2}{4h_2}\left(\frac{\partial^2 \phi_3(x,t)}{\partial t^2}\right)+\frac{I_2^{(2)}h_3}{2h_2^2}\left(\frac{\partial^2 u_3(x,t)}{\partial t^2}\right)$$
$$+\frac{I_2^{(2)}h_3^2}{4h_2^2}\left(\frac{\partial^2 \phi_3(x,t)}{\partial t^2}\right)-\frac{I_1^{(2)}h_3}{2h_2}\left(\frac{\partial^2 u_3(x,t)}{\partial t^2}\right)+\frac{I_2^{(2)}h_1h_3}{4h_2^2}\left(\frac{\partial^2 \phi_1(x,t)}{\partial t^2}\right)+\frac{1}{8}I_0^{(2)}h_3\left(\frac{\partial^2 u_3(x,t)}{\partial t^2}\right)+\frac{1}{8}I_0^{(2)}h_1\left(\frac{\partial^2 u_1(x,t)}{\partial t^2}\right)$$
$$-\frac{1}{16}I_0^{(2)}h_1h_3\left(\frac{\partial^2 \phi_1(x,t)}{\partial t^2}\right) \quad (27d)$$

$$
\begin{aligned}
&A_{55}^{(1)}\left(\frac{\partial\phi_1(x,t)}{\partial x}\right)+A_{55}^{(1)}\left(\frac{\partial^2 w(x,t)}{\partial x^2}\right)+A_{55}^{(3)}\left(\frac{\partial\phi_3(x,t)}{\partial x}\right)+A_{55}^{(3)}\left(\frac{\partial^2 w(x,t)}{\partial x^2}\right)-\frac{A_{55}^{(2)}h_3}{2h_2}\left(\frac{\partial\phi_3(x,t)}{\partial x}\right)\\
&+\frac{A_{55}^{(2)}}{h_2}\left(\frac{\partial u_1(x,t)}{\partial x}\right)-\frac{A_{55}^{(2)}h_1}{2h_2}\left(\frac{\partial\phi_1(x,t)}{\partial x}\right)-\frac{A_{55}^{(2)}}{h_2}\left(\frac{\partial u_3(x,t)}{\partial x}\right)+A_{55}^{(2)}\left(\frac{\partial^2 w(x,t)}{\partial x^2}\right)+A_{11}^{(1)}\left(\frac{\partial w(x,t)}{\partial x}\right)\left(\frac{\partial^2 u_1(x,t)}{\partial x^2}\right)\\
&+\frac{3}{2}A_{11}^{(1)}\left(\frac{\partial w(x,t)}{\partial x}\right)^2\left(\frac{\partial^2 w(x,t)}{\partial x^2}\right)+B_{11}^{(1)}\left(\frac{\partial w(x,t)}{\partial x}\right)\left(\frac{\partial^2\phi_1(x,t)}{\partial x^2}\right)+A_{11}^{(1)}\left(\frac{\partial^2 w(x,t)}{\partial x^2}\right)\left(\frac{\partial u_1(x,t)}{\partial x}\right)\\
&+B_{11}^{(1)}\left(\frac{\partial^2 w(x,t)}{\partial x^2}\right)\left(\frac{\partial\phi_1(x,t)}{\partial x}\right)+A_{11}^{(3)}\left(\frac{\partial w(x,t)}{\partial x}\right)\left(\frac{\partial^2 u_3(x,t)}{\partial x^2}\right)+\frac{3}{2}A_{11}^{(3)}\left(\frac{\partial w(x,t)}{\partial x}\right)^2\left(\frac{\partial^2 w(x,t)}{\partial x^2}\right)\\
&+B_{11}^{(3)}\left(\frac{\partial w(x,t)}{\partial x}\right)\left(\frac{\partial^2\phi_3(x,t)}{\partial x^2}\right)+A_{11}^{(3)}\left(\frac{\partial^2 w(x,t)}{\partial x^2}\right)\left(\frac{\partial u_3(x,t)}{\partial x}\right)+B_{11}^{(3)}\left(\frac{\partial^2 w(x,t)}{\partial x^2}\right)\left(\frac{\partial\phi_3(x,t)}{\partial x}\right)\\
&=I_0^{(1)}\left(\frac{\partial^2 w(x,t)}{\partial t^2}\right)+I_0^{(2)}\left(\frac{\partial^2 w(x,t)}{\partial t^2}\right)+I_0^{(3)}\left(\frac{\partial^2 w(x,t)}{\partial t^2}\right)
\end{aligned}
\tag{27e}
$$

To obtain the frequency equations of the beam, we consider the displacements of the beam to be harmonic [26].

$$u_i(x,t)=U_i(x)e^{i\omega t} \tag{28a}$$

$$\varphi_i(x,t)=\Phi_i(x)e^{i\omega t} \tag{28b}$$

$$w(x,t)=W(x)e^{i\omega t} \tag{28c}$$

Substituting relations (28) in Eqs. (27), the frequency equations of the beam based on Timoshenko theory, are obtained as follows.

$$
\begin{aligned}
&A_{11}^{(1)}\left(\frac{\mathrm{d}^2U_1(x)}{\mathrm{d}x^2}\right)-B_{11}^{(1)}\left(\frac{\mathrm{d}^2\Phi_1(x)}{\mathrm{d}x^2}\right)+\frac{1}{2}A_{55}^{(2)}\frac{h_3}{h_2^2}\left(\frac{\mathrm{d}\Phi_3(x)}{\mathrm{d}x}\right)+\frac{1}{2}A_{55}^{(2)}\frac{h_1}{h_2^2}\Phi_1(x)-\frac{A_{55}^{(2)}}{h_2}\left(\frac{\mathrm{d}W(x)}{\mathrm{d}x}\right)\\
&-\frac{I_2^{(2)}}{h_2^2}U_1(x)\omega^2+\frac{I_2^{(2)}}{h_2^2}U_3(x)\omega^2+\frac{1}{4}I_0^{(2)}U_1(x)\omega^2+\frac{1}{4}I_0^{(2)}U_3(x)\omega^2+\frac{I_1^{(2)}}{h_2}U_1(x)\omega^2+I_0^{(1)}U_1(x)\omega^2\\
&+I_1^{(1)}\Phi_1(x)\omega^2-\frac{1}{8}I_0^{(2)}h_1\Phi_1(x)\omega^2+\frac{1}{8}I_0^{(2)}h_3\Phi_3(x)\omega^2-\frac{1}{2}I_2^{(2)}\frac{h_3}{h_2^2}\Phi_1(x)\omega^2-\frac{1}{2}I_2^{(2)}\frac{h_1}{h_2^2}\Phi_1(x)\omega^2\\
&-\frac{A_{55}^{(2)}}{h_2^2}U_1(x)-\frac{1}{2}I_1^{(2)}\frac{h_1}{h_2}\Phi_1(x)\omega^2+\frac{A_{55}^{(2)}}{h_2^2}U_3(x)-\frac{A_{55}^{(2)}}{h_2^2}U_1(x)=0
\end{aligned}
\tag{29a}
$$

$$
\begin{aligned}
&A_{11}^{(3)}\left(\frac{\mathrm{d}^2U_3(x)}{\mathrm{d}x^2}\right)-B_{11}^{(3)}\left(\frac{\mathrm{d}^2\Phi_3(x)}{\mathrm{d}x^2}\right)-\frac{1}{2}A_{55}^{(2)}\frac{h_3}{h_2^2}\Phi_3(x)-\frac{1}{2}A_{55}^{(2)}\frac{h_1}{h_2^2}\Phi_1(x)+\frac{A_{55}^{(2)}}{h_2}\left(\frac{\mathrm{d}W(x)}{\mathrm{d}x}\right)\\
&+\frac{I_2^{(2)}}{h_2^2}U_3(x)\omega^2-\frac{I_2^{(2)}}{h_2^2}U_1(x)\omega^2+\frac{1}{4}I_0^{(2)}U_1(x)\omega^2+\frac{1}{4}I_0^{(2)}U_3(x)\omega^2-\frac{I_1^{(2)}}{h_2}U_3(x)\omega^2+I_0^{(3)}U_3(x)\omega^2\\
&-I_1^{(3)}\Phi_3(x)\omega^2+\frac{1}{8}I_0^{(2)}h_3\Phi_3(x)\omega^2-\frac{1}{8}I_0^{(2)}h_1\Phi_1(x)\omega^2-\frac{1}{2}I_1^{(2)}\frac{h_3}{h_2}\Phi_3(x)\omega^2+\frac{1}{2}I_2^{(2)}\frac{h_3}{h_2^2}\Phi_3(x)\omega^2\\
&-\frac{A_{55}^{(2)}}{h_2^2}U_3(x)+\frac{1}{2}I_2^{(2)}\frac{h_1}{h_2^2}\Phi_1(x)\omega^2+\frac{A_{55}^{(2)}}{h_2^2}U_1(x)=0
\end{aligned}
\tag{29b}
$$

$$
\begin{aligned}
&-\frac{1}{2}A_{55}^{(2)}\frac{h_1}{{h_2}^2}U_3(x)-\frac{1}{4}A_{55}^{(2)}\frac{h_3h_1}{{h_2}^2}\Phi_3(x)-\frac{1}{2}I_1^{(2)}\frac{h_1}{h_2}U_1(x)\omega^2+\frac{1}{4}I_1^{(2)}\frac{h_1^2}{h_2}\Phi_1(x)\omega^2+\frac{1}{4}I_2^{(2)}\frac{h_3h_1}{{h_2}^2}\Phi_3(x)\omega^2\\
&-\frac{1}{8}I_0^{(2)}h_1U_3(x)\omega^2-\frac{1}{16}I_0^{(2)}h_3h_1\Phi_3(x)+B_{11}^{(1)}\left(\frac{\mathrm{d}^2U_1(x)}{\mathrm{d}x^2}\right)+D_{11}^{(1)}\left(\frac{\mathrm{d}^2\Phi_1(x)}{\mathrm{d}x^2}\right)-A_{55}^{(1)}\Phi_1(x)-A_{55}^{(1)}\left(\frac{\mathrm{d}W(x)}{\mathrm{d}x}\right)\\
&+\frac{1}{2}A_{55}^{(2)}\frac{h_1}{{h_2}^2}U_1(x)-\frac{1}{4}A_{55}^{(2)}\frac{h_1^2}{{h_2}^2}\Phi_1(x)+I_2^{(1)}\Phi_1(x)\omega^2-\frac{1}{2}I_2^{(2)}\frac{h_1}{{h_2}^2}U_1(x)\omega^2+\frac{1}{2}A_{55}^{(2)}\frac{h_1}{h_2}\left(\frac{\mathrm{d}W(x)}{\mathrm{d}x}\right)\\
&+I_1^{(1)}U_1(x)\omega^2+\frac{1}{16}I_0^{(2)}h_1^2\Phi_1(x)\omega^2+\frac{1}{4}I_2^{(2)}\frac{h_1^2}{{h_2}^2}\Phi_1(x)\omega^2+\frac{1}{2}I_2^{(2)}\frac{h_1}{{h_2}^2}U_3(x)\omega^2-\frac{1}{8}I_0^{(2)}h_1U_1(x)\omega^2=0
\end{aligned}
\tag{29c}
$$

$$
\begin{aligned}
&-\frac{1}{4}A_{55}^{(2)}\frac{h_3h_1}{{h_2}^2}\Phi_1(x)+\frac{1}{2}A_{55}^{(2)}\frac{h_3}{h_2}\left(\frac{\mathrm{d}W(x)}{\mathrm{d}x}\right)+I_1^{(3)}U_3(x)\omega^2+I_2^{(3)}\Phi_3(x)\omega^2+\frac{1}{4}I_2^{(2)}\frac{h_3^2}{{h_2}^2}\Phi_3(x)\omega^2\\
&-\frac{1}{2}I_2^{(2)}\frac{h_3}{{h_2}^2}U_1(x)\omega^2+\frac{1}{2}I_2^{(2)}\frac{h_3}{{h_2}^2}U_3(x)\omega^2+\frac{1}{8}I_0^{(2)}h_3U_3(x)\omega^2+\frac{1}{8}I_0^{(2)}h_3U_1(x)\omega^2+\frac{1}{16}I_0^{(2)}h_3^2\Phi_3(x)\omega^2\\
&+\frac{1}{4}I_2^{(2)}\frac{h_3h_1}{{h_2}^2}\Phi_1(x)\omega^2-\frac{1}{4}I_1^{(2)}\frac{h_3^2}{h_2}\Phi_3(x)\omega^2-\frac{1}{2}I_1^{(2)}\frac{h_3}{h_2}U_3(x)\omega^2-\frac{1}{16}I_0^{(2)}h_3h_1\Phi_3(x)\omega^2+B_{11}^{(3)}\left(\frac{\mathrm{d}^2U_3(x)}{\mathrm{d}x^2}\right)\\
&+D_{11}^{(3)}\left(\frac{\mathrm{d}^2\Phi_3(x)}{\mathrm{d}x^2}\right)-A_{55}^{(3)}\Phi_3(x)-A_{55}^{(3)}\left(\frac{\mathrm{d}W(x)}{\mathrm{d}x}\right)-\frac{1}{4}A_{55}^{(2)}\frac{h_3^2}{{h_2}^2}\Phi_3(x)+\frac{1}{2}A_{55}^{(2)}\frac{h_3}{{h_2}^2}U_1(x)-\frac{1}{2}A_{55}^{(2)}\frac{h_3}{{h_2}^2}U_3(x)=0
\end{aligned}
\tag{29d}
$$

$$
\begin{aligned}
&\frac{A_{55}^{(2)}}{h_2}\left(\frac{\mathrm{d}U_1(x)}{\mathrm{d}x}\right)+A_{55}^{(2)}\left(\frac{\mathrm{d}^2W(x)}{\mathrm{d}x^2}\right)+I_0^{(2)}W(x)\omega^2+\frac{9}{8}A_{11}^{(3)}\left(\frac{\mathrm{d}W(x)}{\mathrm{d}x}\right)^2\left(\frac{\mathrm{d}^2W(x)}{\mathrm{d}x^2}\right)+I_0^{(1)}W(x)\omega^2\\
&+\frac{9}{8}A_{11}^{(1)}\left(\frac{\mathrm{d}W(x)}{\mathrm{d}x}\right)^2\left(\frac{\mathrm{d}^2W(x)}{\mathrm{d}x^2}\right)+I_0^{(3)}W(x)\omega^2+A_{55}^{(1)}\left(\frac{\mathrm{d}^2W(x)}{\mathrm{d}x^2}\right)-\frac{A_{55}^{(2)}}{h_2}\left(\frac{\mathrm{d}U_3(x)}{\mathrm{d}x}\right)+A_{55}^{(3)}\left(\frac{\mathrm{d}\Phi_3(x)}{\mathrm{d}x}\right)\\
&+A_{55}^{(3)}\left(\frac{\mathrm{d}^2W(x)}{\mathrm{d}x^2}\right)+A_{55}^{(1)}\left(\frac{\mathrm{d}\Phi_1(x)}{\mathrm{d}x}\right)-\frac{1}{2}A_{55}^{(2)}\frac{h_3}{h_2}\left(\frac{\mathrm{d}\Phi_3(x)}{\mathrm{d}x}\right)-\frac{1}{2}A_{55}^{(2)}\frac{h_1}{h_2}\left(\frac{\mathrm{d}\Phi_1(x)}{\mathrm{d}x}\right)=0
\end{aligned}
\tag{29e}
$$

3 CALCULATION OF THE EQUATIONS OF MOTION IN TERMS OF DISPLACEMENT FIELD YSING GDQM

3.1 Solution procedure

The DQM is a numerical discretization technique for the approximation of derivatives in which very accurate numerical results can be obtained by using just a few grid points with respect to finite differences and finite elements methods. The main idea of the GDQM is that the derivative of a function $f(x)$ at a sample point can be approximated as a weighted linear summation of the function value at all of the sample points in the domain, that is [27].

$$
\frac{\partial^r f(x)}{\partial x^r}=\sum_{j=1}^{n}C_{ij}^{(r)}f(x_i) \tag{30}
$$

where the number of grid points along *x* direction is defined by *n*. Also, C_{ij} is obtained as follows:

$$
C_{ij}^{(1)}=\frac{M(x_i)}{(x_i-x_j)M(x_j)}\quad,\quad i,j=1,2,...,n\ \ and\ \ i\neq j \tag{31a}
$$

$$
C_{ii}^{(1)}=-\sum_{j=1,i\neq j}^{n}C_{ij}^{(1)}\quad,\quad i,j=1,2,...,N \tag{31b}
$$

In which $M(x)$ is defined as:

$$M(x_i)=\prod_{j=1,i\neq j}^{n}(x_i-x_j) \tag{32}$$

And superscript r is the order of derivative. Also, $C^{(r)}$ is the weighting coefficient along x direction which is written as:

$$C_{ij}^{(r)}=r\left(C_{ij}^{(r-1)}C_{ij}^{(1)}-\frac{C_{ij}^{(r-1)}}{(x_i-x_j)}\right)\ ,\quad i,j=1,2,...,n\ ,\ i\neq j\ \ and\ \ 2\leq r\leq n-1 \tag{33a}$$

$$C_{ii}^{(r)}=-\sum_{j-1,i\neq j}^{n}C_{ij}^{(r)}\ ,\quad i,j=1,2,...,n\ and\ 1\leq r\leq n-1 \tag{33b}$$

In order to obtain a better mesh point distribution and increased convergence of solutions, Chebyshev–Gauss–Lobatto technique has been employed as follows:

$$\zeta_i=\frac{1}{2}\left(1-\cos\left(\left(\frac{i-1}{N-1}\right)\pi\right)\right)\ ,\quad i=1,2,...,n \tag{34}$$

Finally, by applying boundary conditions equations into Eq. (29) and using eigenvalue equation in the form of (35), the overall problem will be solved and natural frequency will be calculated.

$$\left[K^{Linear}+\frac{3}{4}K^{Non-linear}(w)\right]_{total}\{w\}=\omega^2\{w\} \tag{35}$$

To solve the problem of nonlinear eigenvalue Eq. (34), an iterative process should be used. For this purpose, in the first step, by neglecting the nonlinear terms, the eigenvalue problem is solved in each case and the linear eigenvector is then appropriately normalized by dividing to the maximum transverse displacement. In the second step, by applying the eigenvector related to the eigenvalues of Eq. (35), the nonlinear vibration equation will be solved. Finally, the eigenvalue problems are solved again to help us obtain the new eigenvalues and eigenvectors. The iterative process continues until the nonlinear frequency values from the two subsequent iterations 'e' and '$e+1$' satisfy the prescribed convergence criteria as:

$$\left|\omega^{e+1}+\omega^{e}\right|/\omega<\varepsilon\ ,\quad \varepsilon=10^{-4} \tag{36}$$

3.2 Equations of motion using GDQM

By applying the Generalized Differential Quadrature Method (GDQM) in the Eqs. (29), the motion equations of the beam based on Timoshenko theory, are obtained as follows:

$$A_{11}^{(1)}\left(\sum_{j=1}^{N}C_{ij}^{(2)}U_{1_j}(x)\right)-B_{11}^{(1)}\left(\sum_{j=1}^{N}C_{ij}^{(2)}\Phi_{1_j}(x)\right)+\frac{1}{2}A_{55}^{(2)}\frac{h_3}{{h_2}^2}\left(\sum_{j=1}^{N}C_{ij}^{(1)}\Phi_{3_j}(x)\right)+\frac{1}{2}A_{55}^{(2)}\frac{h_1}{{h_2}^2}\Phi_{1_i}(x)$$
$$-\frac{A_{55}^{(2)}}{h_2}\left(\sum_{j=1}^{N}C_{ij}^{(1)}W_j(x)\right)-\frac{I_2^{(2)}}{{h_2}^2}U_{1_i}(x)\omega^2+\frac{I_2^{(2)}}{{h_2}^2}U_{3_i}(x)\omega^2+\frac{1}{4}I_0^{(2)}U_{1_i}(x)\omega^2+\frac{1}{4}I_0^{(2)}U_{3_i}(x)\omega^2$$
$$+\frac{I_1^{(2)}}{h_2}U_{1_i}(x)\omega^2+I_0^{(1)}U_{1_i}(x)\omega^2+I_1^{(1)}\Phi_{1_i}(x)\omega^2-\frac{1}{8}I_0^{(2)}h_1\Phi_{1_i}(x)\omega^2+\frac{1}{8}I_0^{(2)}h_3\Phi_{3_i}(x)\omega^2 \tag{37a}$$
$$-\frac{1}{2}I_2^{(2)}\frac{h_3}{{h_2}^2}\Phi_{1_i}(x)\omega^2-\frac{1}{2}I_2^{(2)}\frac{h_1}{{h_2}^2}\Phi_{1_i}(x)\omega^2-\frac{A_{55}^{(2)}}{{h_2}^2}U_{1_i}(x)-\frac{1}{2}I_1^{(2)}\frac{h_1}{h_2}\Phi_{1_i}(x)\omega^2+\frac{A_{55}^{(2)}}{{h_2}^2}U_{3_i}(x)$$
$$-\frac{A_{55}^{(2)}}{{h_2}^2}U_{1_i}(x)=0$$

$$A_{11}^{(3)}\left(\sum_{j=1}^{N}C_{ij}^{(2)}U_{3_j}(x)\right)-B_{11}^{(3)}\left(\sum_{j=1}^{N}C_{ij}^{(2)}\Phi_{3_j}(x)\right)-\frac{1}{2}A_{55}^{(2)}\frac{h_3}{{h_2}^2}\Phi_{3_i}(x)-\frac{1}{2}A_{55}^{(2)}\frac{h_1}{{h_2}^2}\Phi_{1_i}(x)+\frac{A_{55}^{(2)}}{h_2}\left(\sum_{j=1}^{N}C_{ij}^{(1)}W_j(x)\right)$$
$$+\frac{I_2^{(2)}}{{h_2}^2}U_{3_i}(x)\omega^2-\frac{I_2^{(2)}}{{h_2}^2}U_{1_i}(x)\omega^2+\frac{1}{4}I_0^{(2)}U_{1_i}(x)\omega^2+\frac{1}{4}I_0^{(2)}U_{3_i}(x)\omega^2-\frac{I_1^{(2)}}{h_2}U_{3_i}(x)\omega^2+I_0^{(3)}U_{3_i}(x)\omega^2$$
$$-I_1^{(3)}\Phi_{3_i}(x)\omega^2+\frac{1}{8}I_0^{(2)}h_3\Phi_{3_i}(x)\omega^2-\frac{1}{8}I_0^{(2)}h_1\Phi_{1_i}(x)\omega^2-\frac{1}{2}I_1^{(2)}\frac{h_3}{h_2}\Phi_{3_i}(x)\omega^2+\frac{1}{2}I_2^{(2)}\frac{h_3}{{h_2}^2}\Phi_{3_i}(x)\omega^2 \tag{37b}$$
$$-\frac{A_{55}^{(2)}}{{h_2}^2}U_{3_i}(x)+\frac{1}{2}I_2^{(2)}\frac{h_1}{{h_2}^2}\Phi_{1_i}(x)\omega^2+\frac{A_{55}^{(2)}}{{h_2}^2}U_{1_i}(x)=0$$

$$-\frac{1}{2}A_{55}^{(2)}\frac{h_1}{{h_2}^2}U_{3_i}(x)-\frac{1}{4}A_{55}^{(2)}\frac{h_3h_1}{{h_2}^2}\Phi_{3_i}(x)-\frac{1}{2}I_1^{(2)}\frac{h_1}{h_2}U_{1_i}(x)\omega^2+\frac{1}{4}I_1^{(2)}\frac{h_1^2}{h_2}\Phi_{1_i}(x)\omega^2+\frac{1}{4}I_2^{(2)}\frac{h_3h_1}{{h_2}^2}\Phi_{3_i}(x)\omega^2$$
$$-\frac{1}{8}I_0^{(2)}h_1U_{3_i}(x)\omega^2-\frac{1}{16}I_0^{(2)}h_3h_1\Phi_{3_i}(x)+B_{11}^{(1)}\left(\sum_{j=1}^{N}C_{ij}^{(2)}U_{1_j}(x)\right)+D_{11}^{(1)}\left(\sum_{j=1}^{N}C_{ij}^{(2)}\Phi_{1_j}(x)\right)-A_{55}^{(1)}\Phi_{1_i}(x)$$
$$-A_{55}^{(1)}\left(\sum_{j=1}^{N}C_{ij}^{(1)}W_j(x)\right)+\frac{1}{2}A_{55}^{(2)}\frac{h_1}{{h_2}^2}U_{1_i}(x)-\frac{1}{4}A_{55}^{(2)}\frac{h_1^2}{{h_2}^2}\Phi_{1_i}(x)+I_2^{(1)}\Phi_{1_i}(x)\omega^2-\frac{1}{2}I_2^{(2)}\frac{h_1}{{h_2}^2}U_{1_i}(x)\omega^2 \tag{37c}$$
$$+\frac{1}{2}A_{55}^{(2)}\frac{h_1}{h_2}\left(\sum_{j=1}^{N}C_{ij}^{(1)}W_j(x)\right)+I_1^{(1)}U_{1_i}(x)\omega^2+\frac{1}{16}I_0^{(2)}h_1^2\Phi_{1_i}(x)\omega^2+\frac{1}{4}I_2^{(2)}\frac{h_1^2}{{h_2}^2}\Phi_{1_i}(x)\omega^2+\frac{1}{2}I_2^{(2)}\frac{h_1}{{h_2}^2}U_{3_i}(x)\omega^2$$
$$-\frac{1}{8}I_0^{(2)}h_1U_{1_i}(x)\omega^2=0$$

$$-\frac{1}{4}A_{55}^{(2)}\frac{h_3h_1}{{h_2}^2}\Phi_{1_i}(x)+\frac{1}{2}A_{55}^{(2)}\frac{h_3}{h_2}\left(\sum_{j=1}^{N}C_{ij}^{(1)}W_j(x)\right)+I_1^{(3)}U_{3_i}(x)\omega^2+I_2^{(3)}\Phi_{3_i}(x)\omega^2+\frac{1}{4}I_2^{(2)}\frac{h_3^2}{{h_2}^2}\Phi_{3_i}(x)\omega^2$$
$$-\frac{1}{2}I_2^{(2)}\frac{h_3}{{h_2}^2}U_{1_i}(x)\omega^2+\frac{1}{2}I_2^{(2)}\frac{h_3}{{h_2}^2}U_{3_i}(x)\omega^2+\frac{1}{8}I_0^{(2)}h_3U_{3_i}(x)\omega^2+\frac{1}{8}I_0^{(2)}h_3U_{1_i}(x)\omega^2+\frac{1}{16}I_0^{(2)}h_3^2\Phi_{3_i}(x)\omega^2$$
$$+\frac{1}{4}I_2^{(2)}\frac{h_3h_1}{{h_2}^2}\Phi_{1_i}(x)\omega^2-\frac{1}{4}I_1^{(2)}\frac{h_3^2}{h_2}\Phi_{3_i}(x)\omega^2-\frac{1}{2}I_1^{(2)}\frac{h_3}{h_2}U_{3_i}(x)\omega^2-\frac{1}{16}I_0^{(2)}h_3h_1\Phi_{3_i}(x)\omega^2-A_{55}^{(3)}\Phi_{3_i}(x) \tag{37d}$$
$$+B_{11}^{(3)}\left(\sum_{j=1}^{N}C_{ij}^{(2)}U_{3_j}(x)\right)+D_{11}^{(3)}\left(\sum_{j=1}^{N}C_{ij}^{(2)}\Phi_{3_j}(x)\right)-A_{55}^{(3)}\left(\sum_{j=1}^{N}C_{ij}^{(1)}W_j(x)\right)-\frac{1}{4}A_{55}^{(2)}\frac{h_3^2}{{h_2}^2}\Phi_{3_i}(x)$$
$$+\frac{1}{2}A_{55}^{(2)}\frac{h_3}{{h_2}^2}U_{1_i}(x)-\frac{1}{2}A_{55}^{(2)}\frac{h_3}{{h_2}^2}U_{3_i}(x)=0$$

$$\begin{aligned}
&\frac{A_{55}^{(2)}}{h_2}\left(\sum_{j=1}^{N}C_{ij}^{(1)}U_{1_j}(x)\right)+A_{55}^{(2)}\left(\sum_{j=1}^{N}C_{ij}^{(2)}W_j(x)\right)+I_0^{(2)}W_i(x)\omega^2+\frac{9}{8}A_{11}^{(3)}\left(\sum_{j=1}^{N}C_{ij}^{(1)}W_j(x)\right)^2\left(\sum_{j=1}^{N}C_{ij}^{(2)}W_j(x)\right)\\
&+I_0^{(1)}W_i(x)\omega^2+\frac{9}{8}A_{11}^{(1)}\left(\sum_{j=1}^{N}C_{ij}^{(1)}W_j(x)\right)^2\left(\sum_{j=1}^{N}C_{ij}^{(2)}W_j(x)\right)+I_0^{(3)}W_i(x)\omega^2+A_{55}^{(1)}\left(\sum_{j=1}^{N}C_{ij}^{(2)}W_j(x)\right)\\
&-\frac{A_{55}^{(2)}}{h_2}\left(\sum_{j=1}^{N}C_{ij}^{(1)}U_{3_j}(x)\right)+A_{55}^{(3)}\left(\sum_{j=1}^{N}C_{ij}^{(1)}\Phi_{3_j}(x)\right)+A_{55}^{(3)}\left(\sum_{j=1}^{N}C_{ij}^{(2)}W_j(x)\right)+A_{55}^{(1)}\left(\sum_{j=1}^{N}C_{ij}^{(1)}\Phi_{1_j}(x)\right)\\
&-\frac{1}{2}A_{55}^{(2)}\frac{h_3}{h_2}\left(\sum_{j=1}^{N}C_{ij}^{(1)}\Phi_{3_j}(x)\right)-\frac{1}{2}A_{55}^{(2)}\frac{h_1}{h_2}\left(\sum_{j=1}^{N}C_{ij}^{(1)}\Phi_{1_j}(x)\right)=0
\end{aligned} \tag{37e}$$

4 VALIDATION

Comparing the results in terms of natural frequencies presented in the literature [28], demonstrates the effectuality of the developed finite element formulation for a MR fluid sandwich beam. This paper developed the generalized differential quadrature formulation for a MR fluid sandwich beam regardless of the shear deformation and rotary inertia effects of the elastic face layers to simplify the precision of the dynamic properties of thin face layers based on MR fluid sandwich beam. The validation of the GDQ formulation is indicated by comparing the natural frequencies examined in the literature [28].

A thin face layers based on MR fluid sandwich beam with the dimensions of elastic layers 300×30×1 *mm* and an identical thickness of MR fluid layer is considered for this simulation. The considered properties of the basic constituents of FG Sandwich Beam are as follows [28].

Table1
Material and geometrical properties of the FG sandwich beam [28].

Layers	Material	Properties
Elastic Layers	Ceramic (Zro_2)	Young modulus $E_c = 168GPa$
		Poisson ratio $v_c = 0.3$
		Density $\rho_c = 5700kg/m^3$
	Metal (Aluminum)	Young modulus $E_m = 68GPa$
		Poisson ratio $v_m = 0.3$
		Density $\rho_m = 2700kg/m^3$
Magnetorheological Core		Density $\rho_{mc} = 3500kg/m^3$

For the accuracy of the obtained equations and the applied solution method, which in this article is the GDQ method, the evaluated first five natural frequencies corresponding to 0 and 250 (G) under simply supported at both ends in the present work are presented and compared with the references [28] and [29] together in Table 2. It shows a reasonable convergence and accuracy in the results of the present GDQ formulation in which the shear deformation and rotary inertia effects are included as regards the frequencies corresponding to higher modes for both magnetic fields. Validation of linear vibrations for GDQM analysis of a magnetorheological functionally graded beam is performed according to the Table 1 specifications.

$$E_m = 6.8\times10^{10}(pa),\ v_m = v_c = 0.3,\ \rho_m = 2700(kg/m^3),\ \rho_2 = 3500(kg/m^3),\ \rho_c = 5700(kg/m^3),$$
$$h_1 = h_2 = h_3 = 1(mm),\ b = 30(mm),\ L = 300(mm),\ SSB$$

Table2
Linear validation for generalized differential quadrature method analysis of a magnetorheological fluid sandwich beam.

	Natural frequency (*Hz*)					
	B=0			*B*=250(*G*)		
Mode number	Present (GDQM)	Ref [28] (FEM)	Ref [29] (FEM)	Present (GDQM)	Ref [28] (FEM)	Ref [29] (FEM)
1	36.77	40.74	40.31	45.75	51.88	50.92
2	105.23	105.70	103.10	124.85	123.56	120.32
3	210.59	206.51	200.07	235.33	229.01	222.24
4	356.29	344.72	332.45	383.52	369.67	357.33
5	545.65	521.57	501.67	573.86	547.94	528.15

The comparison of the results of the present article with the results of Reference [29] is shown in Table 3. The validation of nonlinear vibrations for GDQ analysis of a magnetorheological functionally graded beam is performed according to the following specifications.

$$E_m = 6.9\times10^{10}\,(pa),\ E_2 = 1.794\times10^{6}(Pa),\ \nu_m = \nu_c = 0.3,\ \nu_2 = 0.3,\ \rho_m = \rho_c = 2766(kg/m^3),$$
$$\rho_2 = 968.1(kg/m^3),\ h_1 = h_3 = 1.524(mm),\ h_2 = 0.127(mm),\ L = 177.8(mm), b = 12.7mm,\ SSB,\ \eta_c = 1$$

Table3
Nonlinear validation for generalized differential quadrature method analysis of a magnetorheological fluid sandwich beam.

w/h	Ω_{NL}/Ω_L		η_{NL}/η_L	
	Ref [30] (FEM)	Present (DQM)	Ref [30] (FEM)	Present (DQM)
0.1	1.092	1.065	0.838	0.801
0.2	1.330	1.297	0.565	0.542
0.4	2.019	1.998	0.245	0.213
0.6	2.816	2.801	0.126	0.107
0.8	3.649	3.632	0.075	0.068
1	4.5	4.487	0.049	0.042

5 NUMERICAL RESULTS AND DISCUSSION

Many parameters such as field intensity, fluid layer thickness, complex shear modulus of the MR fluid, beam geometry, boundary conditions, elastic layer thickness, etc. can greatly affect the properties of a sandwich MR beam. The proposed nonlinear model is used to study the effects of the variations in the magnetic field intensity and the MR fluid layer thickness on the properties of the beam in terms of natural frequencies ratio and the loss factors ratio for different boundary conditions.

5.1 Influences of the magnetic field intensity on natural frequencies and loss factors

Fig. 3 summarizes the influence of variations in the magnetic field intensity on the natural frequencies of a MR fluid sandwich beam based on Timoshenko theory and simply–simply (SSB) condition.

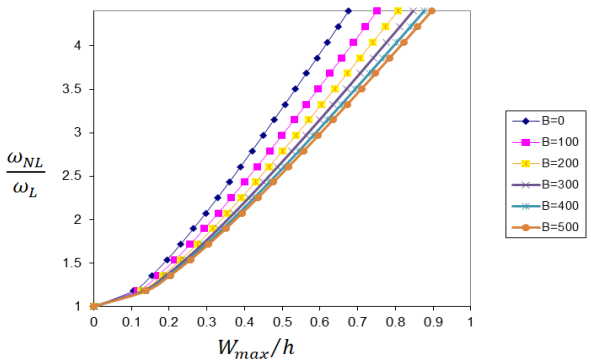

Fig.3
Influence of variations in the magnetic field intensity, on the nonlinear frequency to linear frequency ratio corresponding to maximum deflection to thickness ratio of the magnetorheological beam made of functionally elastic layers.

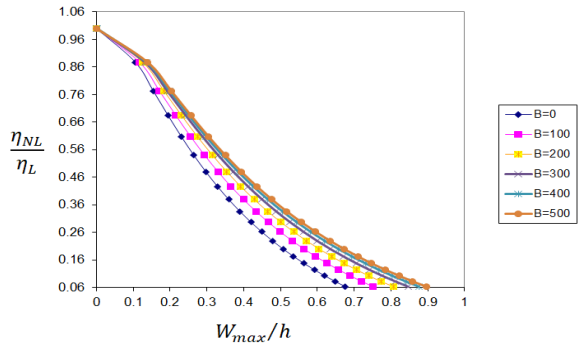

Fig.4
Influence of variations in the magnetic field intensity, on the nonlinear loss factor to linear loss factor ratio corresponding to maximum deflection to thickness ratio of the magnetorheological beam made of functionally elastic layers.

It can be observed that with an increase in the magnetic field intensity, the nonlinear frequency to linear frequency ratio gets lower. Also, at a constant frequency ratio, the maximum deflection to thickness ratio increases with increasing magnetic field intensity. Based on Fig. 4 with an increase in the magnetic field intensity, the nonlinear loss factor to linear loss factor ratio gets higher and at a constant loss factor ratio, the maximum deflection to thickness ratio increases with increasing magnetic field intensity.

5.2 Influences of the power law coefficient in x direction on natural frequencies and loss factors

The variations in the nonlinear frequency to linear frequency ratio and nonlinear loss factor to linear loss factor ratio of the MR beam with simply-simply boundary condition based on Timoshenko theory for different power law coefficients in *x* direction are computed corresponding to the maximum deflection to thickness ratio and are presented in Figs. 5 and 6. The results generally show an increase in the maximum deflection of the beam with decreasing the power law coefficients. Also, with increasing power law exponent, the frequency ratio increases and the loss factor decreases respectively. There is a significant increase in the nonlinear frequency to linear frequency ratio and a significant decrease in nonlinear loss factor to linear loss factor changing of power law coefficient in *x* direction from 0 to 2.

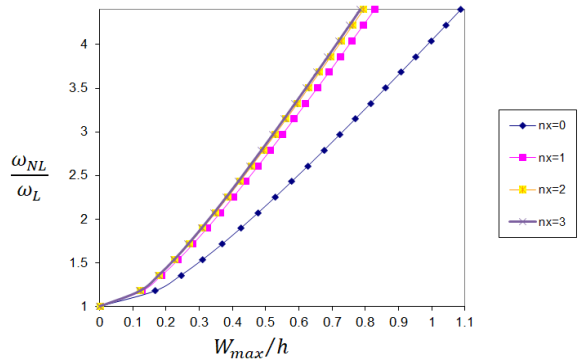

Fig.5
Influence of variations in power law coefficient in *x* direction on the nonlinear frequency to linear frequency ratio corresponding to maximum deflection to thickness ratio of the magnetorheological beam made of functionally elastic layers.

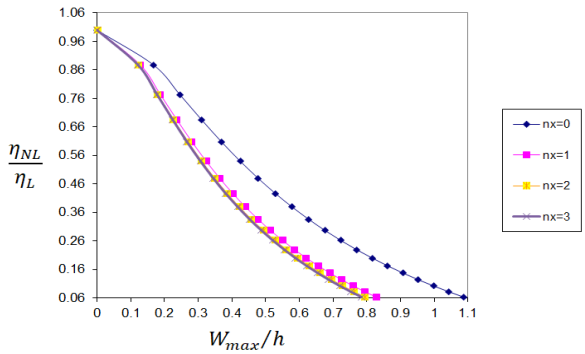

Fig.6
Influence of variations in power law coefficient in *x* direction on the nonlinear loss factor to linear loss factor ratio corresponding to maximum deflection to thickness ratio of the magnetorheological beam made of functionally elastic layers.

5.3 Influences of the MR layer thickness on natural frequencies and loss factors

The variations of frequency and loss factors of the MR beam corresponding to the maximum deflection to thickness ratio at a magnetic field of $B = 500(G)$ for the simply- simply supported end conditions in the different MR layers thickness ratio, have been shown in Figs. 7 and 8.

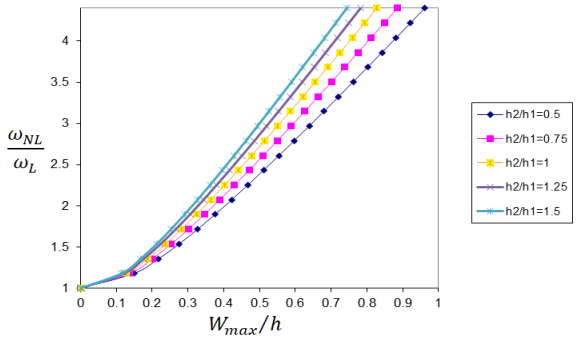

Fig.7
Influence of variations in the MR layer thickness, on the nonlinear frequency to linear frequency ratio corresponding to maximum deflection to thickness ratio of the magnetorheological beam made of functionally elastic layers.

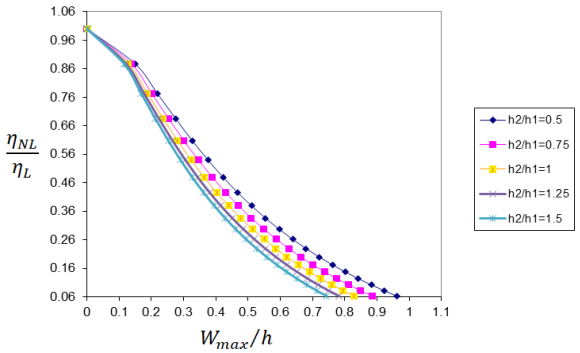

Fig.8
Influence of variations in the MR layer thickness, on the nonlinear loss factor to linear loss factor ratio corresponding to maximum deflection to thickness ratio of the magnetorheological beam made of functionally elastic layers.

The results show that with an increase in the MR layer thickness, the nonlinear frequency to linear frequency ratio gets higher. Also, at a constant frequency ratio, the maximum deflection to thickness ratio decreases with increasing the MR layer thickness (Fig.7). The trend for the nonlinear loss factor to linear loss factor ratio is reversed (Fig.8).

5.4 Influences of the beam length to elastic layer thickness ratio on natural frequencies and loss factor

The variations of frequency and loss factors of the MR beam corresponding to the maximum deflection to thickness ratio at a magnetic field of $B = 500(G)$ for the simply- simply supported end conditions in the different beam length to top layer thickness ratios, have been shown in Figs. 9 and 10.

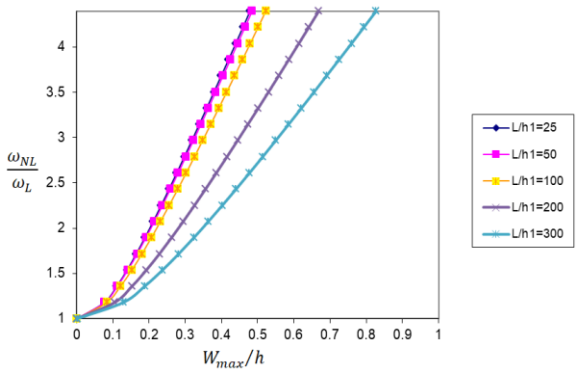

Fig.9
Influence of variations in the different beam length to top layer thickness ratios, on the nonlinear frequency to linear frequency ratio corresponding to maximum deflection to thickness ratio of the magnetorheological beam made of functionally elastic layers.

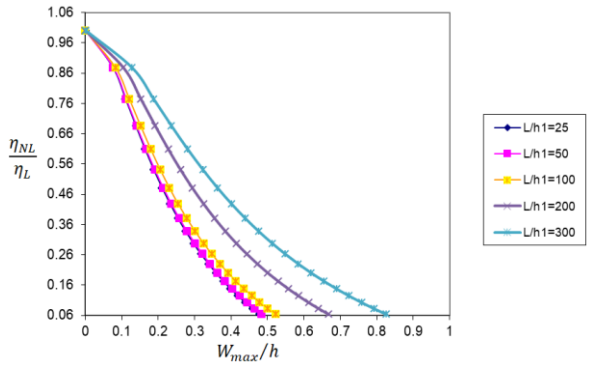

Fig.10
Influence of variations in the different beam length to top layer thickness ratios, on the nonlinear loss factor to linear loss factor ratio corresponding to maximum deflection to thickness ratio of the magnetorheological beam made of functionally elastic layers.

The results obtained from these two diagrams, indicates that increasing the ratio of beam length to the thickness of top layer, the nonlinear frequency to linear frequency ratio will decrease and the nonlinear loss factor to linear loss factor ratio will increase. Also, at a constant frequency ratio, the maximum deflection to thickness ratio increases with increasing the ratio of beam length to the thickness of top layer and at a constant loss factor ratio, the maximum deflection to thickness ratio increases with increasing the ratio of beam length to the thickness of top layer.

5.5 Influences of the boundary conditions on natural frequencies and loss factor

The variations in the nonlinear frequency to linear frequency ratio and nonlinear loss factor to linear loss factor ratio of the functionally graded MR beam based on Timoshenko theory for simply supported-simply supported, simply supported-clamped and clamped-clamped boundary conditions at the magnetic field of $B=0$ corresponding to the maximum deflection to thickness ratio are presented in Figs. 11 and 12.

It can be observed that the simply support-simply support boundary condition has the highest frequency and the clamped-clamped boundary condition has the lowest frequency. It is also observed that the clamped-clamped boundary condition has the highest loss factor and the simply support-simply support boundary condition has the lowest loss factor.

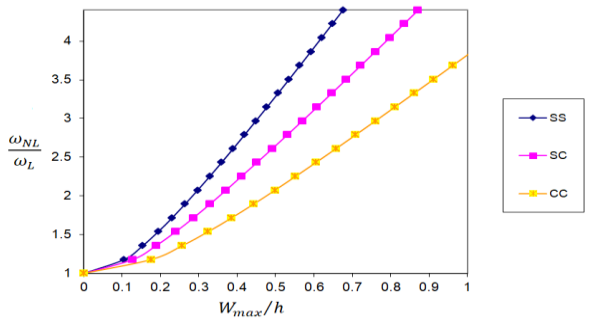

Fig.11
Influence of variations in different boundary conditions, on the nonlinear frequency to linear frequency ratio corresponding to maximum deflection to thickness ratio of the magnetorheological beam made of functionally elastic layers at the magnetic field $B=0$.

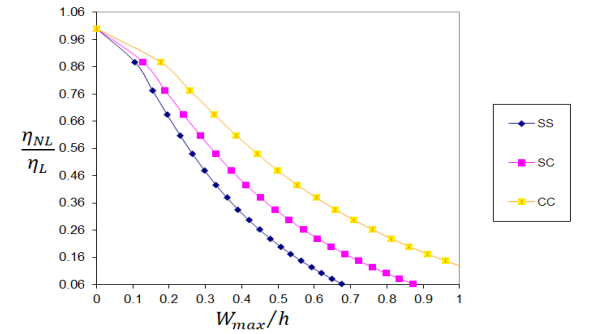

Fig.12
Influence of variations in different boundary conditions, on the nonlinear loss factor to linear loss factor ratio corresponding to maximum deflection to thickness ratio of the magnetorheological beam made of functionally elastic layers at the magnetic field $B=0$.

Also, at a constant frequency ratio and a constant loss factor ratio, the lowest maximum deflection to top layer thickness ratio is related to the simply support-simply support boundary condition and the highest maximum deflection to top layer thickness ratio is related to the clamped-clamped boundary condition.

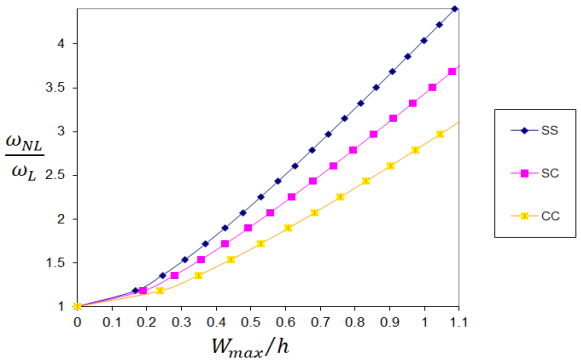

Fig.13
Influence of variations in different boundary conditions, on the nonlinear frequency to linear frequency ratio corresponding to maximum deflection to thickness ratio of the magnetorheological beam made of functionally elastic layers at the power law coefficient $n_x = 0$.

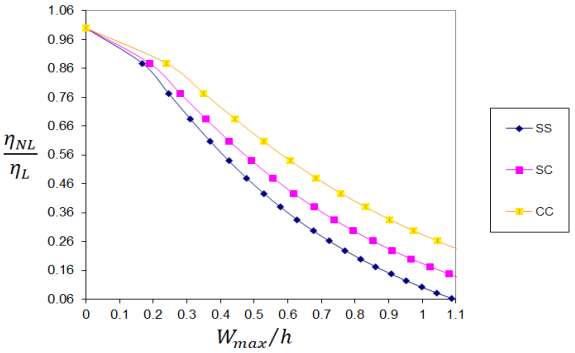

Fig.14
Influence of variations in different boundary conditions, on the nonlinear loss factor to linear loss factor ratio corresponding to maximum deflection to thickness ratio of the magnetorheological beam made of functionally elastic layers at the power law coefficient $n_x = 0$.

Figs.13 and 14 summarize the variations in the nonlinear frequency to linear frequency ratio and nonlinear loss factor to linear loss factor ratio of the functionally graded MR beam based on Timoshenko theory for simply supported-simply supported, simply supported-clamped and clamped-clamped boundary conditions at the power law coefficient $n_x = 0$ corresponding to the maximum deflection to thickness ratio. It can be observed that the simply support-simply support boundary condition has the highest frequency and the clamped-clamped boundary condition has the lowest frequency. It is also observed that the clamped-clamped boundary condition has the highest loss factor and the simply support-simply support boundary condition has the lowest loss factor. Also, at a constant frequency ratio and a constant loss factor ratio, the lowest maximum deflection to top layer thickness ratio is related to the simply support-simply support boundary condition and the highest maximum deflection to top layer thickness ratio is related to that the clamped-clamped boundary condition.

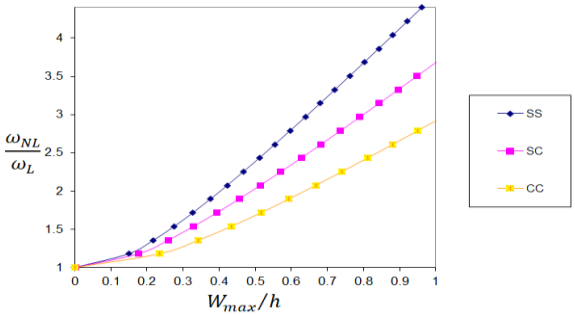

Fig.15
Influence of variations in different boundary conditions, on the nonlinear frequency to linear frequency ratio corresponding to maximum deflection to thickness ratio of the magnetorheological beam made of functionally elastic layers at the thickness ratio $h_2/h_1 = 0.5$.

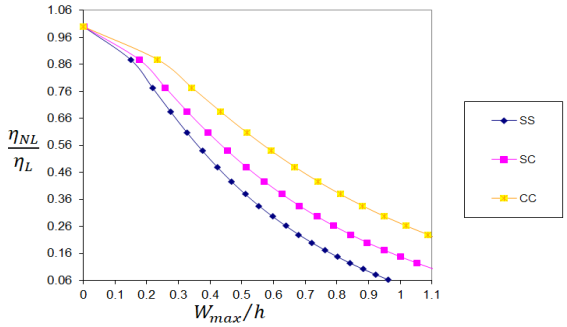

Fig.16
Influence of variations in different boundary conditions, on the nonlinear loss factor to linear loss factor ratio corresponding to maximum deflection to thickness ratio of the magnetorheological beam made of functionally elastic layers at the thickness ratio $h_2/h_1 = 0.5$.

Figs.15 and 16 summarize the variations in the nonlinear frequency to linear frequency ratio and nonlinear loss factor to linear loss factor ratio of the functionally graded MR beam based on Timoshenko theory for simply supported-simply supported, simply supported-clamped and clamped-clamped boundary conditions at the thickness ratio $h_2/h_1 = 0.5$ corresponding to the maximum deflection to thickness ratio. It can be observed that the simply support-simply support boundary condition has the highest frequency and the clamped-clamped boundary condition has the lowest frequency. It is also observed that the clamped-clamped boundary condition has the highest loss factor and the simply support-simply support boundary condition has the lowest loss factor. Also, at a constant frequency ratio and a constant loss factor ratio, the lowest maximum deflection to top layer thickness ratio is related to the simply support-simply support boundary condition and the highest maximum deflection to top layer thickness ratio is related to that the clamped-clamped boundary condition.

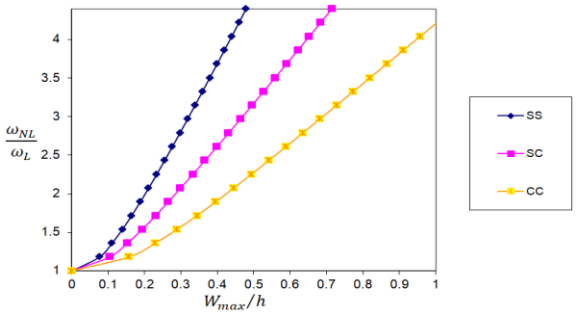

Fig.17
Influence of variations in different boundary conditions, on the nonlinear frequency to linear frequency ratio corresponding to maximum deflection to thickness ratio of the magnetorheological beam made of functionally elastic layers at the beam length to top layer thickness $L/h_1 = 25$.

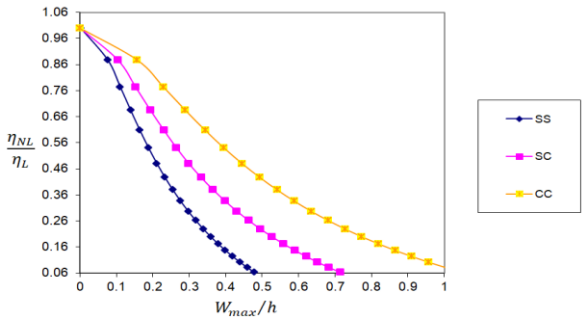

Fig.18
Influence of variations in different boundary conditions, on the nonlinear loss factor to linear loss factor ratio corresponding to maximum deflection to thickness ratio of the magnetorheological beam made of functionally elastic layers at the beam length to top layer thickness $L/h_1 = 25$.

Figs.17 and 18 summarize the variations in the nonlinear frequency to linear frequency ratio and nonlinear loss factor to linear loss factor ratio of the functionally graded MR beam based on Timoshenko theory for simply supported-simply supported, simply supported-clamped and clamped-clamped boundary conditions at the beam length to top layer thickness $L/h_1 = 25$ corresponding to the maximum deflection to thickness ratio. It can be observed that the simply support-simply support boundary condition has the highest frequency and the clamped-clamped boundary condition has the lowest frequency. It is also observed that the clamped-clamped boundary condition has the highest loss factor and the simply support-simply support boundary condition has the lowest loss factor. Also, at a constant frequency ratio and a constant loss factor ratio, the lowest maximum deflection to top layer thickness ratio is related to the simply support-simply support boundary condition and the highest maximum deflection to top layer thickness ratio is related to that the clamped-clamped boundary condition.

6 CONCLUSIONS

In this paper, the analysis of nonlinear free vibrations of functionally graded beams with Magnetorheological fluid as core is investigated. It is assumed that the beam is located on Simply-Simply(SS), Clamped-Simply(CS) and Clamped–Clamped(CC) supports, and is made of three layers including Constraining Layer, Magnetorheological (MR) fluid and Base Layer. The governing equations of the beam are derived using the Hamilton's principle. To obtain the vibrational frequencies and modeling of composite layers, the theory of Timoshenko beam with von Karman geometric nonlinearity are used by the Generalized Differential Quadrature (GDQ) method. In core modeling, only shear strain energy is considered. The shear strain in core is expressed by writing the continuity relationships in the layers. The complex shear modulus of the magnetorheological material in the pre-yield region is modeled with the complex shear modulus, which is a function of the magnetic field intensity. The validity of the relationships is shown by comparing the results in terms of natural frequencies with the results in other articles. The effects of magnetic field intensity, dimensional ratio, core thickness and constraining layer thickness on natural frequency and modal loss factor related to different beam modes for the three mentioned SS, CS and CC boundary conditions have been investigated. The results show the impact of physical and geometrical parameters regarding the natural frequency and modal loss factor of the sandwich beam with different modes. The manageable capabilities of MR fluid were perused through conducting various parametric studies.

The main points of this study are outlined as follows:

- In all three boundary conditions, by increasing the strength of the magnetic field (B), the natural frequencies ratio $\left(\frac{\omega_{NL}}{\omega_L}\right)$ would be decreased and loss factor ratio $\left(\frac{\eta_{NL}}{\eta_L}\right)$ would be increased.
- In all three boundary conditions, by increasing the length of the beam (L), the natural frequencies ratio $\left(\frac{\omega_{NL}}{\omega_L}\right)$ would be decreased and loss factor ratio $\left(\frac{\eta_{NL}}{\eta_L}\right)$ would be increased.
- In all three boundary conditions, by increasing the power law coefficient $\left(n_x\right)$, the natural frequencies ratio $\left(\frac{\omega_{NL}}{\omega_L}\right)$ would be increased and loss factor ratio $\left(\frac{\eta_{NL}}{\eta_L}\right)$ would be decreased.
- In all three boundary conditions, by increasing the MR layer thickness $\left(\frac{h_2}{h_1}\right)$, the natural frequencies ratio $\left(\frac{\omega_{NL}}{\omega_L}\right)$ would be increased and loss factor ratio $\left(\frac{\eta_{NL}}{\eta_L}\right)$ would be decreased.
- Regarding the comparison of boundary conditions, it can be said that in different values of magnetic field strength, in different values of power law coefficient, in different values of MR layer thickness and in different values of beam length, the simply supported boundary condition has the highest natural frequencies ratio $\left(\frac{\omega_{NL}}{\omega_L}\right)$ and the lowest loss factors ratio $\left(\frac{\eta_{NL}}{\eta_L}\right)$.
- Regarding the comparison of boundary conditions, it can be said that in different values of magnetic field strength, in different values of power law coefficient, in different values of MR layer thickness and in different values of beam length, the clamped supported boundary condition has the highest loss factors ratio $\left(\frac{\eta_{NL}}{\eta_L}\right)$ and the lowest natural frequencies ratio $\left(\frac{\omega_{NL}}{\omega_L}\right)$.
- The comparison of the analysis of GDQ and FEM methods shows that the frequency values and loss factor obtained from GDQ method were obtained with a small percentage difference compared to FEM method. This shows the accuracy and precision of the GDQ method.

ACKNOWLEDGMENT

I gratefully appreciate my co-supervisors, Dr. Saeed Jafari Mehrabadi and Professor. Mohammad Mahdi Najafizadeh for their great supervision and crucial guidance from the beginning of the paper as well as providing me continuous support and encouragement throughout the research.

REFERENCES

[1] Ashtiani M., Hashemabadi S.H., Ghaffari A., 2015, A review on the magnetorheological fluid preparation and stabilization, *Journal of Magnetism and Magnetic Materials* **374**: 711-715.

[2] Allahverdizadeh A., Eshraghi I., Mahjoob M.J., Nasrollahzadeh N., 2014, Nonlinear vibration analysis of FGER sandwich beams, *International Journal of Mechanical Sciences* **78**:167-176.

[3] Aguib S., Nour A., Benkoussas B., Tawfiq I., Djedid T., Chikh N., 2016, Numerical simulation of the nonlinear static behavior of composite sandwich beams with a magnetorheological elastomer core, *Composite Structures* **139**:111-119.

[4] Acharya S., Allien V.J., Kumar H., 2021, Dynamic behavior of sandwich beams with different compositions of magnetorheological fluid core, *International Journal* of *Smart* and *Nano Materials* **12**:88-106.

[5] Nayak B., Dwivedy S.K., Murthy K.S.R.K., 2013, Vibration analysis of a three-layer magnetorheological elastomer embedded sandwich beam with conductive skins using finite element method, *Proceedings of the Institution of Mechanical Engineers, Part C: Journal of Mechanical Engineering Science* **227**: 714-729.

[6] Navazi H.M., Bornassi S., Haddadpour H., 2017, Vibration analysis of a rotating magnetorheological tapered sandwich beam, *International Journal of Mechanical Sciences* **122**: 308-317.

[7] Marynowski K., 2012, Dynamic analysis of an axially moving sandwich beam with viscoelastic core, *Composite Structures* **94**: 2931-2936.

[8] Wei K., Bai Q., Meng G., Ye L., 2011, Vibration characteristics of electrorheological elastomer sandwich beams, *Smart Materials and Structures* **20**: 055012.

[9] Allahverdizadeh A., Mahjoob M.J., Eshraghi I., Asgharifard-S. P., 2012, Effects of electrorheological fluid core and functionally graded layers on the vibration behavior of a rotating composite beam, *Meccanica* **47**: 1945-1960.

[10] Allahverdizadeh A., Mahjoob M.J., Eshraghi I., Nasrollahzadeh N., 2013, On the vibration behavior of functionally graded electrorheological sandwich beams, *International Journal of Mechanical Sciences* **70**: 130-139.

[11] Ke L.L., Yang J., Kitipornchai S., 2010, An analytical study on the nonlinear vibration of functionally graded beams, *Meccanica* **45**: 743-752.

[12] Elmaguiri M.N., Haterbouch M., Bouayad A., Oussouaddi O., 2015, Geometrically nonlinear free vibration of functionally graded beams, *Journal of Materials and Environmental Science* **6**: 3620-3633.

[13] Taeprasartsit S., 2015, Nonlinear free vibration of thin functionally graded beams using the finite element method, *Journal of Vibration and Control* **21**: 29-46.

[14] Sheng G.G., Wang X., 2018, Nonlinear vibration of FG beams subjected to parametric and external excitations, *European Journal of Mechanics; A/Solids* **71**: 224-234.

[15] Barari A., Kaliji H.D., Ghadimi M., Domairry G., 2011, Non-linear vibration of Euler-Bernoulli beams, *Latin American Journal of Solids and Structures* **8**(2):139-148.

[16] Sınır S., Çevik M., Sınır B.G., 2018, Nonlinear free and forced vibration analyses of axially functionally graded Euler-Bernoulli beams with non-uniform cross-section, *Composites Part B: Engineering* **148**: 123-131.

[17] Hemmatnezhad M., Ansari R., Rahimi G.H., 2013, Large-amplitude free vibrations of functionally graded beams by means of a finite element formulation, *Applied Mathematical Modelling* **37**: 8495-84504.

[18] Gunda J.B., Gupta R.K., Janardhan G.R., Rao G.V., 2010, Large amplitude free vibration analysis of Timoshenko beams using a relatively simple finite element formulation, *International Journal of Mechanical Sciences* **52**: 1597-1604.

[19] Ebrahimi F., Zia M., 2015, Large amplitude nonlinear vibration analysis of functionally graded Timoshenko beams with porosities, *Acta Astronautica* **116**: 117-125.

[20] Chen D., Kitipornchai S., Yang J., 2016, Nonlinear free vibration of shear deformable sandwich beam with a functionally graded porous core, *Thin-walled Structures* **107**: 39-48.

[21] Ghorbanpour Arani A., Kolahchi R., Haghighi S., Mosallaie Barzoki A.A., 2013, Nonlinear viscose flow induced nonlocal vibration and instability of embedded DWCNC via DQM, *Journal of Mechanical Science and Technology* **27**: 21-31.

[22] Ghaitani M.M., Ghorbanpourarani A., Khademizadeh H., 2014, Nonlinear vibration and instability of embedded viscose-fluid-conveying pipes using DQM, *Advanced Design and Manufacturing Technology* **7**: 45-51.

[23] Yeh J.Y., 2013, Vibration analysis of sandwich rectangular plates with magnetorheological elastomer damping treatment, *Smart Materials and Structures* **22**: 035010.

[24] Rajamohan V., Rakheja S., Sedaghati R., 2010, Vibration analysis of a partially treated multi-layer beam with magnetorheological fluid, *Journal of Sound* and *Vibration* **329**: 3451-3469.

[25] Zhong Z., Wu L., Chen W., 2012, *Mechanics of Functionally Graded Materials and Structures*, Springer.

[26] Kang J.H., 2014, An exact frequency equation in closed form for Timoshenko beam clampled at both ends, *Journal of Sound* and *Vibration* **333**: 3332-3337.
[27] Shafiei N., Kazemi M., Ghadiri M., 2016, Nonlinear vibration behavior of a rotating nanobeam under thermal stress using Eringen's nonlocal elasticity and DQM, *Applied Physics A: Materials Science & Processing* **122**: 123265759.
[28] Rajamohan V., Sundararaman V., Govindarajan B., 2013, Finite element vibration analysis of a magnetorheological fluid sandwich beam, *Procedia Engineering* **64**: 603-612.
[29] Rajamohan V., Sedaghati R., Rakheja S., 2010, Vibration analysis of a multi-layer beam containing magnetorheological fluid, *Smart Materials and Structures* **19**: 015013.
[30] Bilasse M., Daya E.M., Azrar L., 2010, Linear and nonlinear vibrations analysis of viscoelastic sandwich beams, *Journal of Sound* and *Vibration* **329**: 4950-4969.